Semiannual Technical Report

Nitride Semiconductors for Ultraviolet Detection

Supported under Grant #N00014-92-J-1720
Office of the Chief of Naval Research
Report for the period 7/1/94–12/31/94

R. F. Davis, K. Linthicum, B. Perry, L. Smith and W. Weeks
Materials Science and Engineering Department
North Carolina State University
Campus Box 7907
Raleigh, NC 27695-7907

December, 1994

REPORT DOCUMENTATION PAGE

Form Approved
OMB No. 0704-0188

1. AGENCY USE ONLY *(Leave blank)*	2. REPORT DATE	3. REPORT TYPE AND DATES COVERED
	December, 1994	Semiannual Technical 7/1/94–12/31/94

4. TITLE AND SUBTITLE

Nitride Semiconductors for Ultraviolet Detection

5. FUNDING NUMBERS

s400018srr01
1114SS
N00179
N66005
4B855

6. AUTHOR(S)

Robert F. Davis

7. PERFORMING ORGANIZATION NAME(S) AND ADDRESS(ES)

North Carolina State University
Hillsborough Street
Raleigh, NC 27695

8. PERFORMING ORGANIZATION REPORT NUMBER

N00014-92-J-1720

9. SPONSORING/MONITORING AGENCY NAMES(S) AND ADDRESS(ES)

Sponsoring: ONR, Code 314, 800 N. Quincy, Arlington, VA 22217-5660
Monitoring: Administrative Contracting Officer, Regional Office Atlanta
101 Marietta Tower, Suite 2805
101 Marietta Street
Atlanta, GA 30332-0490

10. SPONSORING/MONITORING AGENCY REPORT NUMBER

11. SUPPLEMENTARY NOTES

12a. DISTRIBUTION/AVAILABILITY STATEMENT

Approved for Public Release; Distribution Unlimited

12b. DISTRIBUTION CODE

13. ABSTRACT ***(Maximum 200 words)***

Monocrystalline, undoped, high resistivity GaN thin films have been grown on (6H)-SiC(0001) wafers via organometallic vapor phase epitaxy (OMVPE) employing a high-temperature monocrystalline AlN buffer layer using a cold-wall, vertical pancake-style reactor with triethylgallium (TEG), triethylaluminum (TEA) and ammonia. The surface morphologies of films deposited on both vicinal and on-axis, Si- and C-polar planes of SiC(0001) are described. Controlled n-type Si-doping in GaN has been achieved with carrier concentrations from ~10^{17} to 10^{20} cm^{-3}. SEM and TEM of the latter films revealed high microstructural quality. Photoluminescence (PL) of the undoped GaN revealed a sharp donor-bound exciton peak at 357.2 nm, with a FWHM of 4 meV. The defect peaks in these samples were very weak. The Si-doped GaN exhibited a strong PL emission at 358 nm due to donor-to-valence band transitions. Mg-doped GaN emitted strong blue light with a peak wavelength of 426 nm. Cathodoluminescence measurements of $Al_xGa_{1-x}N$ were also successful, with strong emission at the band-edge. An ammonia cracker cell, has also been designed and installed in the gas source MBE to replace the ECR plasma source to minimize film damage and to enhance film quality and growth rate. Low resistivity Al, Cu_3Ge, and TiN ohmic contacts have been achieved on Si-doped, n-type GaN. Au and a Au/Mg/Au layered structure exhibited ohmic behavior on p-GaN when annealed at high temperature or in the as-deposited condition, respectively. As-deposited Pt formed ohmic contacts to Mg:GaN. Microstructural characterization of the Al/n-GaN and Au/p-GaN contact systems revealed that interfacial reactions occurred during annealing and markedly affected contact performance.

14. SUBJECT TERMS

gallium nitride, GaN, organometallic vapor phase epitaxy, OMVPE, thin films, scanning electron microscopy, transmission electron microscopy, photoluminescence, cathodoluminescence, Si-doping, ammonia cracker cell, gas source MBE, ohmic contacts, Al, Cu_3Ge, TiN, Pt, annealing, interfacial reactions

15. NUMBER OF PAGES

41

16. PRICE CODE

17. SECURITY CLASSIFICATION OF REPORT	18. SECURITY CLASSIFICATION OF THIS PAGE	19. SECURITY CLASSIFICATION OF ABSTRACT	20. LIMITATION OF ABSTRACT
UNCLAS	UNCLAS	UNCLAS	SAR

Table of Contents

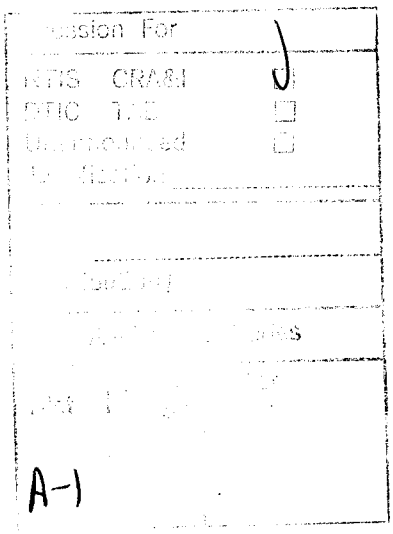

I. Introduction

Continued development and commercialization of optoelectronic devices, including light-emitting diodes and semiconductor lasers produced from III–V gallium arsenide-based materials, has also generated interest in the much wider bandgap semiconductor mononitride materials containing aluminum, gallium, and indium. The majority of the studies have been conducted on pure gallium nitride thin films having the wurtzite structure, and this emphasis continues to the present day. Recent research has resulted in the fabrication of p–n junctions in wurtzitic gallium nitride, the deposition of cubic gallium nitride, as well as the fabrication of multilayer heterostructures and the formation of thin film solid solutions. Chemical vapor deposition (CVD) has usually been the technique of choice for thin film fabrication. However, more recently these materials have also been deposited by plasma-assisted CVD and reactive and ionized molecular beam epitaxy.

The program objectives achieved in this reporting period have been (1) the growth of monocrystalline, undoped, high resistivity GaN thin films on α(6H)-SiC(0001) wafers via organometallic vapor phase epitaxy (OMVPE), (2) controlled n-type Si-doping in these films with carrier concentrations from ~10^{17} to 10^{20} cm^{-3}, (3) microstructural, photo-luminescence and cathodoluminescence of GaN and Al_xGa_{1-x} films, (4) the development of a novel NH_3 cracker cell for gas source MBE to reduce film damage and (5) development of low resistivity ohmic contacts for n- and p-type GaN and their chemical and microstructural characterization as a function of annealing temperature and time.

The procedures, results, discussions of these results and conclusions of these studies are summarized in the following sections with reference to appropriate SDIO/ONR reports for details. Note that each major section is self-contained with its own figures, tables and references.

II. Deposition, Doping and Characterization of OMVPE Grown GaN on Various SiC(0001) Substrates using High-temperature Monocrystalline AlN Buffer Layers

A. Introduction

The potential semiconductor and optoelectronic applications of the wide bandgap III-V nitrides has prompted significant research into their growth and development. GaN (wurtzite structure), the most studied in this group, has a bandgap of 3.4 eV and forms continuous solid solutions with both AlN (6.2 eV) and InN (1.9 eV). As such, materials with engineered bandgaps are envisioned for optoelectronic devices tunable from the visible to deep UV frequencies. An AlGaN/InGaN/AlGaN double heterostructure-base blue LED is now commercially available in Japan. The relatively strong atomic bonding of these materials also points to their potential use in high-power and high-temperature devices.

Single crystal wafers of GaN do not exist [1]. Sapphire(0001) is the most commonly used substrate, although its lattice parameter and coefficient of thermal expansion are different than that of GaN. The use of low-temperature (450°C-600°C) buffer layers of AlN [2-5] or GaN film quality and surface morphology. Undoped GaN is typically n-type. To date, p-type behavior has been achieved in chemically vapor deposited Mg- or Zn-doped GaN using post-growth treatments of either low-energy electron beam irradiation [8] or via thermal annealing in a N_2 atmosphere [9, 10]. Acceptor-type behavior has been obtained directly in molecular beam epitaxially grown films [11].

In the present research high quality monocrystalline GaN thin films have been grown on n-type α(6H)-SiC(0001) wafers employing high-temperature (HT) monocrystalline AlN buffer layers via organometallic vapor phase epitaxy (OMVPE) in a cold-wall, pancake-style reactor. This is the first known report of the use of *high-temperature* buffer layers to improve subsequent GaN growth. GaN film growth on vicinal and on-axis wafers as well as the different Si- and C-polar planes of SiC(0001) were also investigated. Triethylgallium (TEG), triethylaluminum (TEA) and ammonia (NH_3) were used as reactants. Controlled n-type Si-doping of GaN using silane (SiH_4) was demonstrated. Doping with bis-cyclopentadienyl-magnesium (Cp_2Mg) produced deep blue emission in the PL spectrum. The heteroepitaxial growth of GaN and AlN on SiC was characterized using scanning electron microscopy (SEM), transmission electron microscopy (TEM), photoluminescence (PL) spectroscopy and Hall-effect measurements. Atomic dopant levels were measured using secondary ion mass spectrometry (SIMS). The following sections describe the experimental procedures, detail the results, provide a discussion and conclusions regarding this research and outline future research plans and goals.

B. Experimental Procedure

GaN thin films were grown on Si-face and C-face, vicinal and on-axis SiC(0001) substrates at 950°C. Vicinal wafers are SiC(0001) 3°-4° off-axis toward the <11$\bar{2}$0>. High-temperature monocrystalline AlN buffers layers were employed in this study. The as-received SiC wafers were cut into 7.1mm squares. The SiC pieces were degreased, dipped into a 10% HF solution for 10 minutes to remove the thermally grown oxide layer and blown dry with N_2 before being loaded onto the pancake-style, SiC-coated graphite susceptor. The reactor was evacuated to less than 3×10^{-5} Torr for one hour prior to initiating growth. The continuously rotating susceptor was rf inductively heated to 1100°C in 3 SLM of flowing H_2 diluent. Hydrogen was also used as the carrier gas for the various metalorganic precursors. Once this growth temperature was reached and stabilized, AlN deposition was started by flowing TEA and NH_3 into the reactor at 23.6 μmol/min and 1.5 SLM, respectively. The system pressure during growth was 45 torr. The AlN was grown for 30 minutes resulting in a thickness of 100 nm. With the NH_3 and H_2 flowing at their prescribed rates, the TEA flow was terminated. The temperature was decreased to 950°C, and the system pressure was increased to 90 torr for the GaN growth. The flow rate of TEG was maintained at 24.76 μmol/min. The growth rate for GaN was 0.9 μm/hr. Si-doped GaN samples were grown by additionally flowing SiH_4 (8.2 ppm in N_2 balance) at flow rates between 0.05 nmol/min and 15 nmol/min. Likewise, Cp_2Mg was used as the Mg-doping source.

The structural, microstructural, optical and electrical characteristics of the epitaxial GaN thin films were analyzed using several techniques. SEM was performed on a JEOL 6400FE operating at 5 kV. Conventional and high resolution TEM was performed on a Topcon EM-002B microscope operating at 200 kV. The photoemission properties of the GaN films were determined using low-temperature ($T \approx 7K$) PL obtained using a 15 mW He-Cd laser (325 nm) as the excitation source. The Si-doped GaN films were characterized by Hall-effect measurements using the Van der Pauw geometry. Thermally evaporated Al was used as the contacts to these films with only linear regions of the current-voltage (I-V) curves being used for taking the Hall-effect measurements.

C. Results and Discussion

TEM Microstructures. For growth on SiC(0001) substrates, the use of high-temperature monocrystalline AlN buffers layers dramatically improves the resulting GaN film quality. The GaN film and the HT-AlN buffer layer are monocrystalline as determined by TEM selected area diffraction. The high quality of the GaN on vicinal $SiC(0001)_{Si}$ using a HT-AlN buffer layer is apparent in the cross-sectional TEM micrograph shown in Fig. 1. The stacking fault density is noticeably very low. Also, the usually observed double positioning boundaries (DPBs) common in GaN films grown by other CVD and MBE techniques are not observed. Internal

stresses resulting from heteroepitaxial growth appear to be relaxed at the very strained GaN/AlN interface. From initial plan view TEM analysis, the defect density of the GaN film shown in Fig. 1 deposited on a vicinal $SiC(0001)_{Si}$ wafer using a HT-AlN buffer layer is roughly $1e^8$ cm^{-2}.

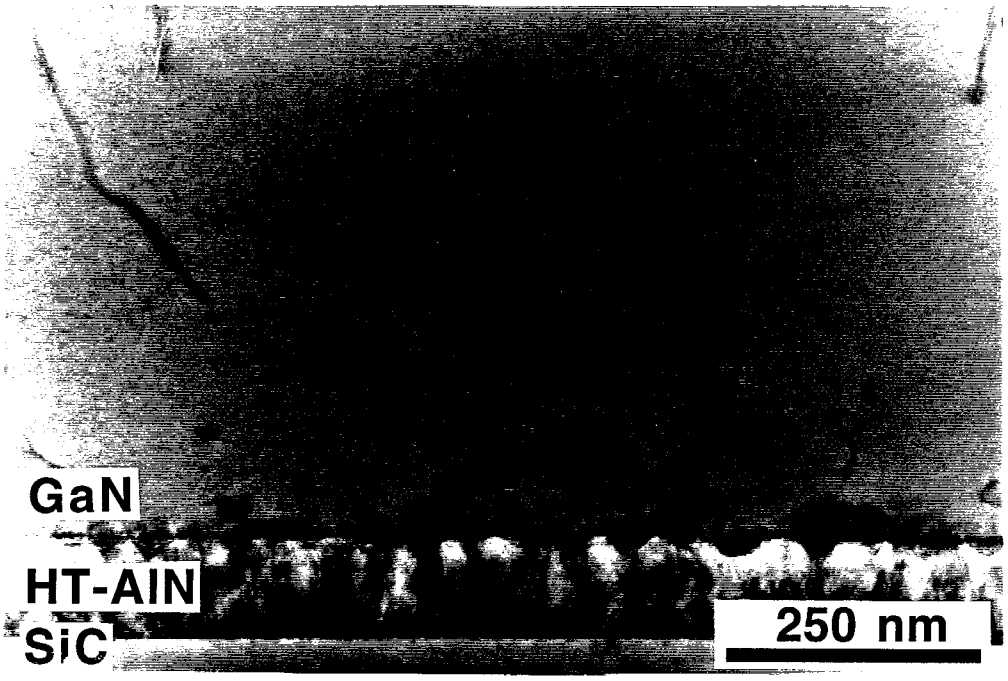

Figure 1. TEM micrograph of GaN grown on vicinal $SiC(0001)_{Si}$ at 950°C by OMVPE employing a high-temperature (1100°C) monocrystalline AlN buffer layer.

Figure 2 shows a cross-sectional TEM micrograph of GaN/HT-AlN deposited on an on-axis $SiC(0001)_{Si}$ substrate. The dislocations appear to traverse the GaN perpendicular to the SiC(0001) interface. The dislocations in the vicinal sample shown in Fig. 1 seem to have more random orientations. The dislocation mechanism in both samples is under investigation, beginning with a Burgers vector analysis.

Because of the relative closeness in lattice parameters and coefficients of thermal expansion between wurtzitic AlN and (6H)-SiC, monocrystalline AlN can be deposited directly on SiC at high temperatures. Thus, there is no apparent need to deposit a low-temperature amorphous AlN buffer layer requiring subsequent thermal annealing for growth on SiC(0001) substrates.

HT-ALN Buffer Layer Surface Morphology. In several experiments, four different SiC wafer types were simultaneously used for GaN film growth employing the HT-AlN buffer layer technique. These substrates were on- and off-axis $SiC(0001)_{Si}$ as well as on- and off-axis $SiC(000\bar{1})_C$. As observed via SEM, the surfaces of the AlN buffer layers on the vicinal and on-axis C-face wafers were very textured with apparent small hexagonal hillocks. This growth

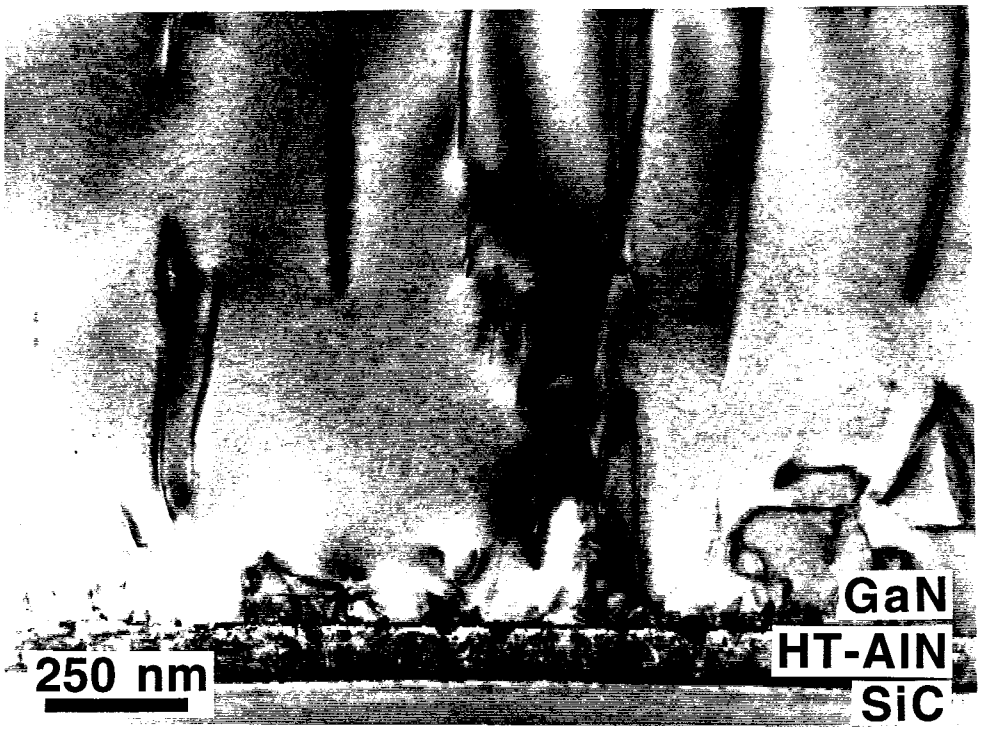

Figure 2. TEM micrograph of GaN grown on an on-axis $SiC(0001)_{Si}$ substrate at 950°C by OMVPE employing a high-temperature (1100°C) monocrystalline AlN buffer layer.

template yielded similar hexagonal hillocks on the surface of the subsequently grown GaN film layer. However, the HT-AlN grown on the vicinal and on-axis $SiC(0001)_{Si}$ had a rather flat and even surface morphology. However, many small pits (approximately 500Å across) were observed on the AlN surfaces when using both Si-face wafer types. By increasing the AlN deposition temperature from 1100°C to 1200°C for the Si-face substrates, the pit density decreased. This decrease was more appreciable in the on-axis SiC(0001) sample than in the vicinal SiC(0001) sample.

GaN Film Surface Morphology. The GaN deposited on the HT-AlN (1100°C) buffer layer on the on-axis $SiC(0001)_{Si}$ substrate had a very smooth and flat surface morphology as shown in Fig. 3. Some random pinholes were observed on the otherwise featureless surface. The cause of these pinholes is believed to be submicron particulate contamination of the growth surface. These particles may be from residual contamination in the reaction chamber or be generated by parasitic gas phase reactions. The surface morphology of the GaN on the vicinal $SiC(0001)_{Si}$ wafer shown in Fig. 4 was also rather smooth with only random pinholes. However, a slightly textured surface was observable apparently resulting from the step and terrace features of the vicinal SiC substrate.

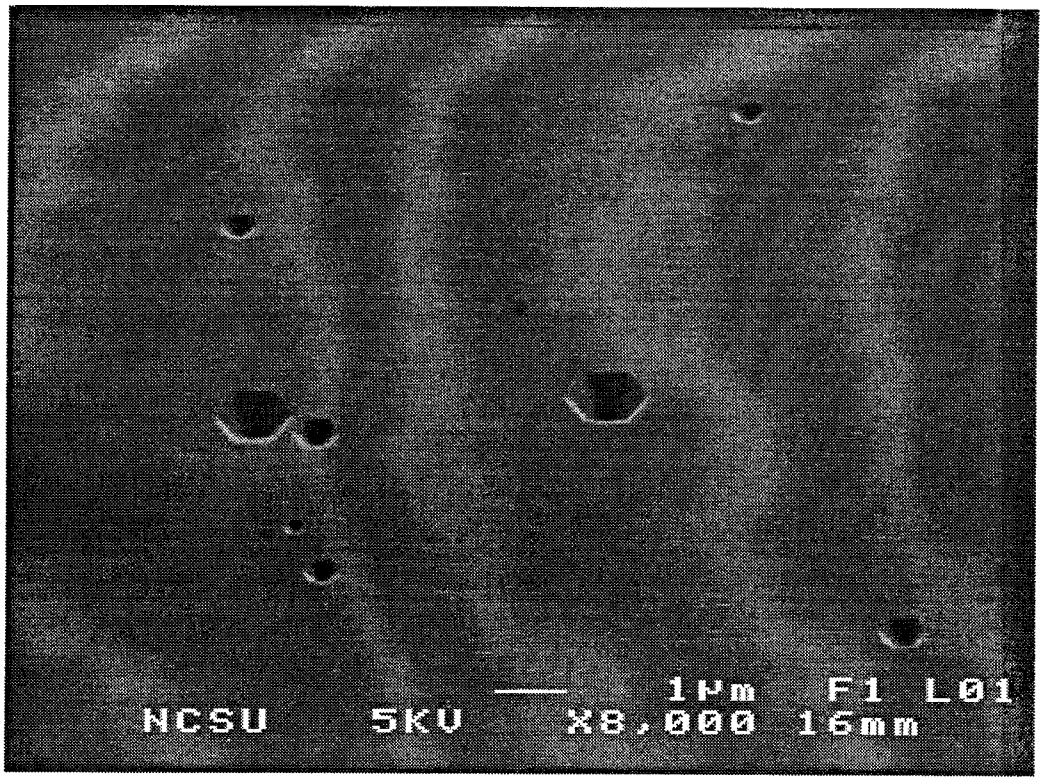

Figure 3. SEM micrograph of GaN deposited on an on-axis $SiC(0001)_{Si}$ substrate using a high-temperature AlN buffer layer.

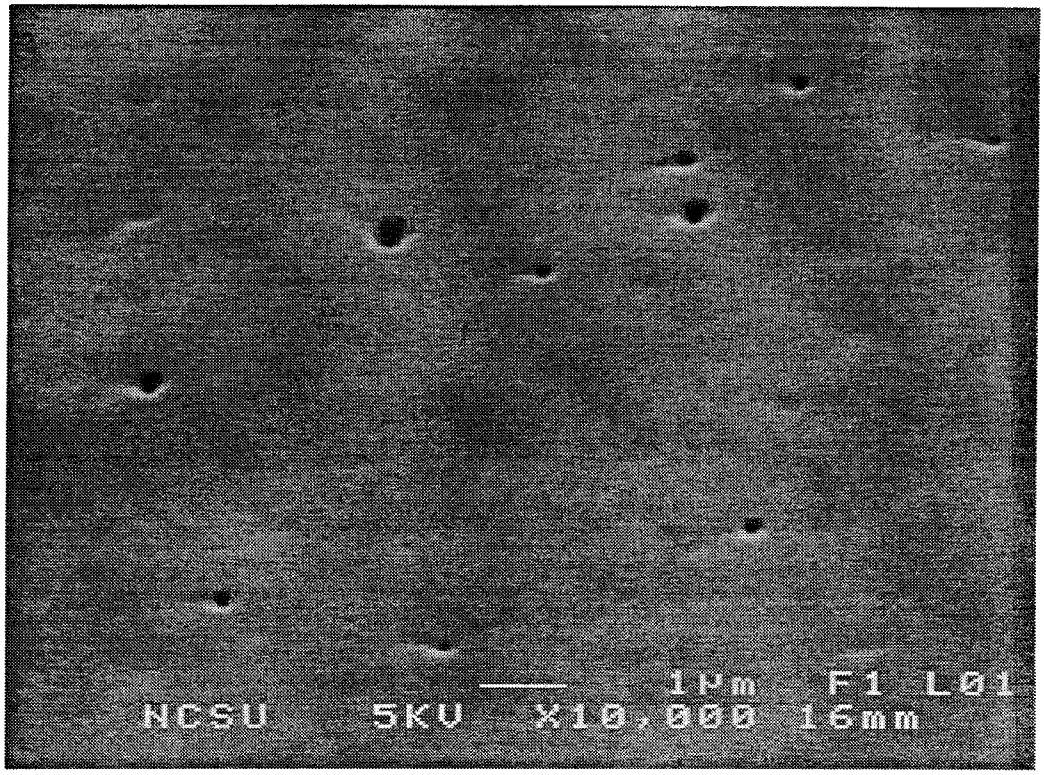

Figure 4. SEM micrograph of GaN deposited on vicinal $SiC(0001)_{Si}$ using a high-temperature AlN buffer layer.

Photoluminescence. Low-temperature PL was performed on the various samples. The spectra of the GaN on both vicinal and on-axis $SiC(0001)_{Si}$ revealed strong band-edge emission at 3.47 eV. For the GaN on the vicinal sample only two weak defect peaks were observed at 3.26 eV and 2.2 eV, respectively (Fig. 5). However, the spectrum from the GaN sample on the on-axis substrate showed defect peaks at 3.26 eV, 3.0 eV and rather intense yellow emission at 2.2 eV (Fig. 6). Similar variations in the PL spectra also were observed for GaN films grown on the vicinal and on-axis $SiC(000\bar{1})_C$ substrates. The causes of the PL spectral differences are under investigation.

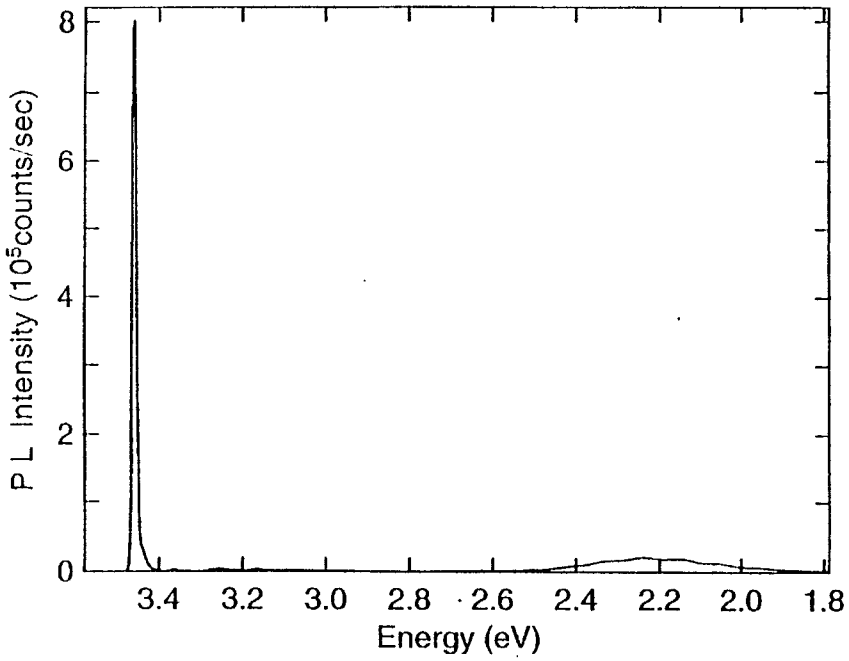

Figure 5. Low-temperature PL of GaN on vicinal $SiC(0001)_{Si}$ with a high-temperature AlN buffer layer.

Si-doping in GaN. Undoped high quality GaN grown on a HT-AlN buffer layer on SiC(0001) is resistive as deposited. However, GaN was controllably n-type doped with Si from a SiH_4 source for net carrier concentrations ranging from approximately $1e^{17}$ cm^{-3} to $1e^{20}$ cm^{-3}. The net carrier concentrations and room temperature mobilities versus SiH_4 flow rate are plotted in Fig. 7. As determined by Hall-effect measurements using the Van der Pauw geometry with thermally evaporated Al contacts, Si-doped GaN films with a net carrier concentration of n_D-n_A = $2e^{17}cm^{-3}$ had a resulting room temperature mobility of μ = 375 $cm^2/V{\cdot}s$.

Mg-doping in GaN. GaN was also doped with Mg using Cp_2Mg. For a magnesium atomic concentration of [Mg] = $6.1e^{19}$ cm^{-3} as determined using a Mg ion-implanted GaN SIMS

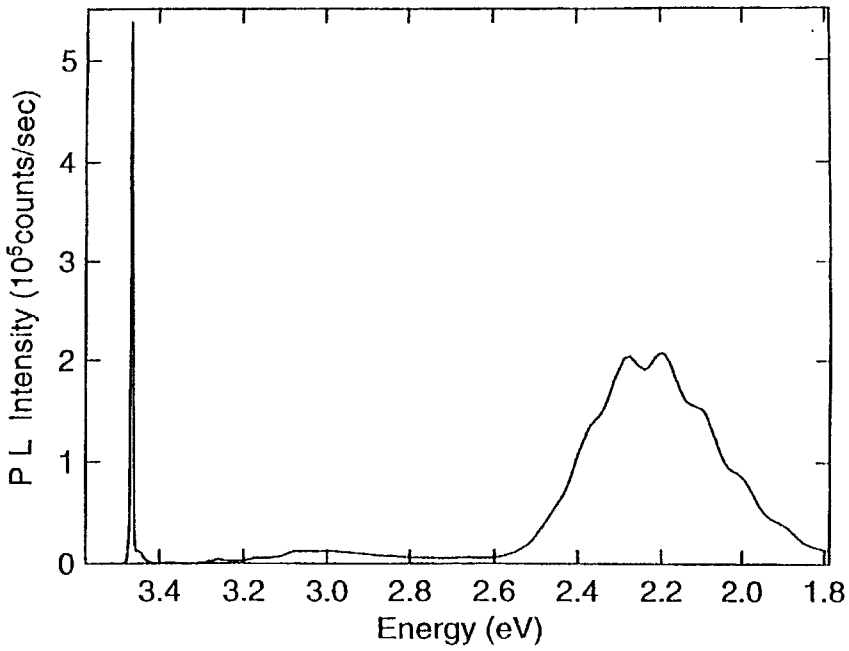

Figure 6. Low-temperature PL of GaN on an on-axis $SiC(0001)_{Si}$ substrate with a high-temperature AlN buffer layer.

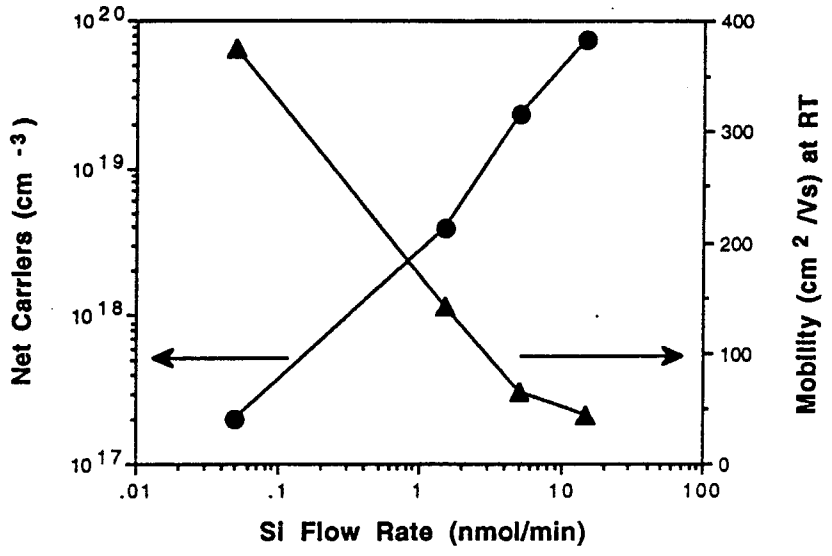

Figure 7. Net carrier concentration and room temperature mobilities in n-type Si-doped GaN as a function of SiH_4 flow rate.

standard, low-temperature PL revealed strong deep blue emission centered at 426 nm (Fig. 8). However, sufficiently ohmic contacts could not be obtained as is necessary for making Hall-effect measurements. Attempts will be made to measure the hole carrier concentrations in Mg-doped GaN films using a Hg-probe C-V system.

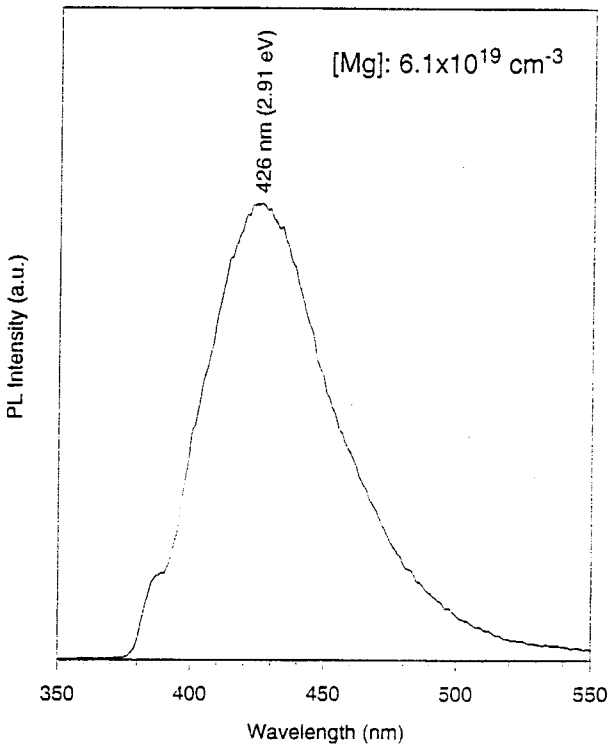

Figure 8. Low-temperature PL of Mg-doped GaN. For a magnesium atomic concentration of [Mg] = $6.1e^{19}$ cm^{-3} strong deep blue emission is observed at 426 nm.

D. Conclusions

High quality GaN thin films have been deposited on vicinal and on-axis α(6H)-$SiC(0001)_{Si}$ substrates using high-temperature monocrystalline AlN buffer layers. The photoemission properties of the GaN on the vicinal SiC substrate were superior to those on the on-axis substrate. Controlled n-type Si-doping of GaN was demonstrated for net carrier concentrations ranging from $1e^{17}$ cm^{-3} to $1e^{20}$ cm^{-3}. Optically active Mg-doped GaN was also observed.

E. Future Research Plans and Goals

Reliable and consistent p-type doping of GaN must be obtained. Thus the role of hydrogen passivation needs further investigation. Once p-type conduction in GaN has been verified, pn-junctions will be fabricated and tested. Concurrently, film growth in the InGaN system must be undertaken for use as the active layer in bright-blue LEDs and laser diodes (LDs).

Continued improvements in film quality in the AlGaN system must occur for use in double heterostructure devices. Also, attempts will be made to controllably dope InGaN and AlGaN n- and p-type. Ultimately, both UV and bright-blue LEDs will be demonstrated, as well as microelectronic devices such as MESFETs and MOSFETs.

F. References

1. R. F. Davis, Physica B **185** (1993) 1.
2. S. Yoshida, S. Misawa and S. Gonda, Appl. Phys. Lett., **42** (1983) 427.
3. S. Yoshida, S. Misawa and S. Gonda, J. Vac. Sci. Technol., **B1** (1983) 250.
4. H.I. Amano, N. Sawaki, I. Akasaki and Y. Toyoda, Appl. Phys. Lett., **48** (1986) 353.
5. I. Akasaki, H.I. Amano, Y. Koide, K. Hiramatsu and N. Sawaki, J. Cryst. Growth, **98** (1989) 209.
6. T. Lei, M. Fanciulli, R.J. Molnar and T.D. Moustakas, Appl. Phys. Lett., **59** (1991) 944.
7. S. Nakamura, M. Senoh and T. Mukai, Jpn. J. Appl. Phys., **30** (1991) L1708.
8. H. Amano, M. Kito, K. Hiramatsu and I. Akasaki, Jpn. J. Appl. Phys., **28** (1989) L2112.
9. S. Nakamura, T. Mukai, M. Senoh and N. Iwasa, Jpn. J. Appl. Phys., **31** (1992) L139.
10. S. Nakamura, N. Iwasa, M. Senoh and T. Mukai, Jpn. J. Appl. Phys., **31** (1992) 1258.
11. C. Wang and R.F. Davis, Appl. Phys. Lett., **63** (1993) 990.

III. Nitride Devices and Use of NH_2 for Film Growth

A. Introduction

AlN, GaN and InN thin films are presently grown by various techniques including MOVPE, RF sputtering, and electron cyclotron resonance (ECR) plasma assisted GSMBE. We are continuing to use the last technique to determine the optimal growth parameters for the binary compounds, selected solid solutions of these compounds and multilayer heterostructures of these materials in terms of microstructure and optical and electrical properties. Discussions with other users of ECR plasmas [1] and our own results have led us to be concerned that, as a result of the low bond strength of the surface and near-surface atoms of GaN and InN, there is an increased potential for point defect damage and resulting electrical compensation in these materials. This damage would arise from the interaction of high energy N species with the surface and near-surface regions of these materials during deposition. This is especially true if the plasma power is increased to enhance the flux of the reactive species. Recent research has shown that GaN films grown at higher microwave powers exhibit degraded electrical and luminescent properties as compared to films grown at lower microwave power levels [2-5]. An alternative method of producing atomic nitrogen that minimizes or eliminates the undesirable production of high energy ionic nitrogen is needed. To address this concern, we are currently collaborating with Effusion Science Inc. regarding the design of a novel high-temperature ammonia-cracking source. This report presents the design and development of the high temperature ammonia cracking source for production of high fluxes of atomic nitrogen as an alternative to the ECR source in GSMBE.

B. Experimental Procedure

The ammonia cracking source manufactured by Effusion Science Inc. has been installed in the sleeve of our currently unused MBE effusion cell (2.25" diameter). Nitride-grade ammonia will be source gas and will be further purified by a Nanochem ammonia purifier prior to entering the cracker cell. After entering the cracker cell, the ammonia will decompose by means of a single bounce delivery off of a wide-area catalytic rhenium filament. Al, Ga, and In fluxes will be provided by the normal MBE effusion cells. AlN, GaN, InN, and their solid solutions will be grown at various temperatures and pressures on SiC and Sapphire to optimize the growth rate and film microstructure. A quadrupole mass spectrometer will be used to determine the efficiency and feasibility of producing the required nitrogen flux needed for III-V nitride film growth.

C. Discussion

The use of cracking ammonia as a source of nitrogen is not new to the field of III-V nitride growth. It is the current method used in growth techniques such as MOCVD and MOVPE

where ammonia is cracked on the surface of the substrate, requiring relatively higher growth temperatures to achieve efficient nitrogen production. Asahi Chemical Industry Co. has recently reported the use of NH_3 in their GSMBE. Reactive molecular beam epitaxy has also used the cracking of ammonia on the substrate as a nitrogen source. Another technique recently used was hot filament enhanced CVD [6,7]. In this process, it is surmised that the catalyzed film growth is initiated through the decomposition of ammonia and subsequent production of NH radicals by a heated tungsten filament. These products trigger further reactions which react with the metalorganic gas to form precursors to film deposition. These precursors then decompose on the heated substrate resulting in film growth [7]. The decomposition of ammonia on various filament surfaces at high temperatures has shown that the two primary reactions that occur are:

$$NH_3 + M \rightarrow NH_2 + H + M \quad 1)$$

$$NH_3 + H \rightarrow NH_2 + H_2 \quad 2)$$

In the case of the catalyzed CVD growth, reaction 2 is enhanced by the addition of hydrogen to the reaction chamber between the tungsten filament and the heated substrate to aid in the production of NH_2. It is the secondary reactions, primarily the formation of NH radicals, that next occur which are responsible for precursor formation with the metalorganic mentioned above [6-8]. Examples of these secondary reactions include:

$$NH_2 + H \rightarrow NH + H_2 \quad 3)$$

$$NH_2 + NH_2 \rightarrow NH + NH_3. \quad 4)$$

Ammonia Gas Cracker. The ammonia will enter the cracker cell and decompose primarily to NH_2 by means of a single interaction with a wide-area catalytic Re filament [6,7]. This process will limit the formation of N_2. Rhenium was chosen for two reasons: (1) rhenium catalysts are exceptionally resistant to passivation from gases such as nitrogen [9] and (2) hydrogen atoms have been detected in ammonia decomposition reactions on rhenium filaments heated to high temperatures approaching 2000 K [10]. Therefore it should not be necessary to add hydrogen from some other source to aid in the production of NH_2. Secondary reactions on the substrate surface will produce NH radicals which are highly reactive with the group III species and result in film growth.

D. Future Research Plans and Goals

Over the next few months we will be testing the ammonia cracker cell and the gas delivery system. Preliminary work will concentrate on optimizing the growth of films by this source of nitrogen. These films will be compared to films grown presently by modified (ECR) GSMBE.

Once we have established that this source of nitrogen is practical for film growth, we will employ the technique for development of optical devices.

E. References

1. S.Strite, IBM Research Report #83986, March 28, 1994 and private discussions.
2. R. J. Molnar, and T. D. Moustakas, J. Appl. Phys. **76** (8), 4587 (1994).
3. R. C. Powell, N. E. Lee, Y. W. Kim, and J. E. Greene, J. Appl. Phys. **73**, 189 (1993).
4. M. E. Lin, B. Sverdlov, G. L. Zhou, and H. Morkoc, Appl. Phys. Lett. **62**, 3479 (1993).
5. R.Singh, R. J. Molnar, M. S. Unlu, and T. D. Moustakas, Appl. Phys. Lett. **64**, 336 (1994)
6. J. L.Dupuie and E. Gulari, Appl. Phys. Lett. **59**, 549 (1991).
7. J. L.Dupuie and E. Gulari, J. Vac. Sci. Technol. A **10** (1), 18 (1991).
8. G. S. Selwyn and M. C. Lin, Chemical Physics **67**, 213 (1982).
9. Handbook of Chemistry and Physics **73**, 4-24 (1992).
10. S. N. Foner and R. L. Hudson, J. Chem. Phys. **80** (9), 4013 (1984).

IV. Luminescence Studies of GaN, AlN, InN and Their Solid Solutions

A. Introduction

Luminescence is the emission of photons due to excited electrons in the conduction band decaying to their original energy levels in the valance band. The wavelength of the emitted light is directly related to the energy of the transition, by E=hν. Thus, the energy levels of a semiconductor, including radiative transitions between the conduction band, valance band, and exciton, donor, and acceptor levels, can be measured.[1,2] Various methods exist to excite the electrons, including photoluminescence (photon excitation), and cathodoluminesence (electron-beam excitation). In each technique, signal intensity is measured at specific wavelength intervals using a monochromator and a detector. The intensity versus wavelength (or energy) plot can then be used to identify the characteristic energy band gap and exciton levels (intrinsic luminescence) of the semiconductor, and the defect energy levels (extrinsic luminescence) within the gap.[1]

Both photo- and cathodoluminescence analysis has been performed on AlN, GaN, InN and their solid solutions.[3-20] Much of the work has been in measuring the low temperature luminescence of GaN. High quality, unintentionally doped GaN exhibits a strong donor-bound exciton peak at 357.3 nm (3.47 eV).[16] Defect peaks due to donor-acceptor (DA) transitions and accompanying phonon replicas are also prevalent, with peak wavelengths at 380.3, 391.2 and 402.9 nm. The identity of the acceptor is not clear. A deep emission at 540 nm (2.2 eV) is also common in GaN. Currently the source of this emission is not know, although various models exist to explain it.[19,20] It is of utmost importance to limit the defect transitions, as it can reduce the transition probability of the near-gap emission.

Although undoped GaN is always n-type, recent advances in film growth have lowered the carrier concentration to $10^{16}/cm^3$. For device applications it is important to have a high carrier concentration at a controlled level. Common dopants for n-type doping of GaN include Si and Ge. Nakamura, *et al.* found that for Si-doped GaN two peaks dominate the spectrum.[12] The first is a UV emission peak at 380 nm. The second peak is the deep level (DL) emission previously discussed; this transition is enhanced by Si-doping. Conflicting results were shown by Murakami, *et al.*, who saw a band edge peak at 358 nm dominate their spectrum.[8] The DL emission at 540 nm in their samples was very weak.

The development of light emitting diodes (LEDs) and laser diodes using GaN-based materials has been limited by the difficulty in obtaining quality p-type films.[12] Common dopants include Zn, Cd, and Mg.[3] Recent work has proven successful, with low resistivity Mg-doped GaN obtained by thermal annealing or low energy electron beam irradiation

(LEEBI) as a post-growth process step. The luminescence from these films typically show a broad peak located at 450 nm, with no emission near the band-edge.

Work on AlN and $Al_xGa_{1-x}N$ has been limited by the energy gap of 6.2 eV for AlN. This corresponds to a wavelength (200 nm) that is lower than most of the optical light sources. An excimer laser using the ArF line (193 nm) could possibly be used, although very little work on this has been done to date. Cathodoluminescence of AlN is possible, however, and most of the results have been obtained via this method.[16-18]. $Al_xGa_{1-x}N$ with low amounts of Al can also be investigated using frequency doubled and tripled lasers that have lines down to 260 nm.

B. Experimental Procedures

A combined photo- and cathodoluminesence system is used to measure the luminescence from the III-V nitrides. A schematic view is shown in Fig. 1, and a block diagram is shown in Fig. 2. Each sample is attached to a cryostat that allows for a test temperature range of 8 to 400 K. A McPherson model 219 vacuum monochromator with a focusing mirror chamber is used to collect the emitted light. The focal length of the monochromator is .5 m, with a wavelength resolution of .04 nm at 313.1 nm for a 1200 G/mm grating. A photon counting detection scheme is used to measure the light intensity, with a photomultiplier tube (PMT) used that has a wavelength range of 180-650 nm. A GaAs PMT that is efficient from 185-930 nm will be added to the system shortly.

A Liconix He-Cd laser is the photoexcitation source. It is a continuous wavelength laser that operates at a wavelength of 325 nm (3.8 eV), with a power of 15 mW. It is used for PL of GaN and $In_xGa_{1-x}N$, but a lower wavelength source is needed to test the full range of $Al_xGa_{1-x}N$ solid solutions. A pulsed excimer laser is proposed as the other optical source; it operates at wavelengths of 193 nm (6.4 eV) and 248 nm (5.0 eV).

A Kimball Physics electron gun is used for cathodoluminesence measurements. It has maximum beam voltage of 10 keV and a maximum beam current of 450 μA. By varying the beam voltage it is possible to perform depth-resolved spectroscopy.

The beam blanking capability of the electron gun will allow for time-delay studies of the semiconductors.

C. Results and Discussion

Photoluminescence measurements were performed on GaN films grown via OMVPE on vicinal α(6H)-SiC(0001)$_{Si}$ wafers. The buffer layer for each sample was AlN. All of the tests were performed at 8 K, unless otherwise noted.

The photoluminescence of undoped GaN grown at 950 °C is shown in Fig. 3. The sample thickness was .68 μm. The peak at 357.2 nm is attributed to the recombination of excitons at neutral donors. The FWHM of this peak, 4 meV, indicates the high quality of the sample. The

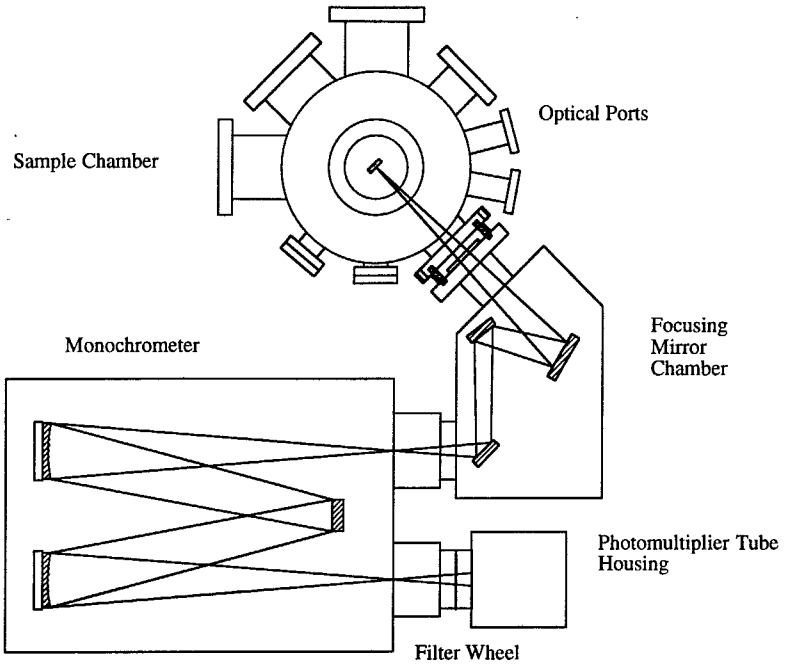

Figure 1. Schematic view of combined photo- and cathodoluminescence system.

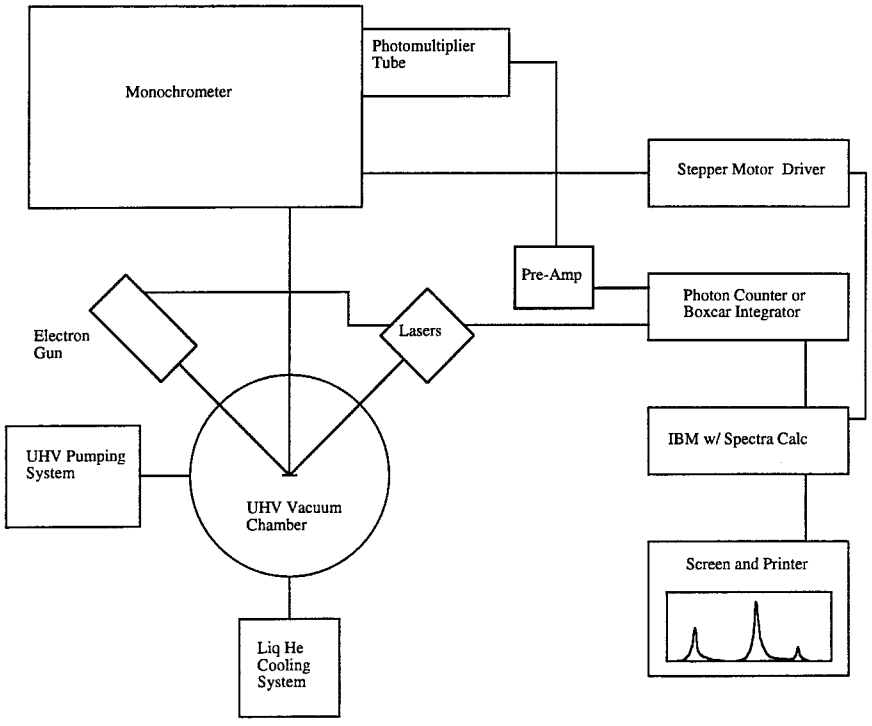

Figure 2. Block diagram of combined photo- and cathodoluminescence system.

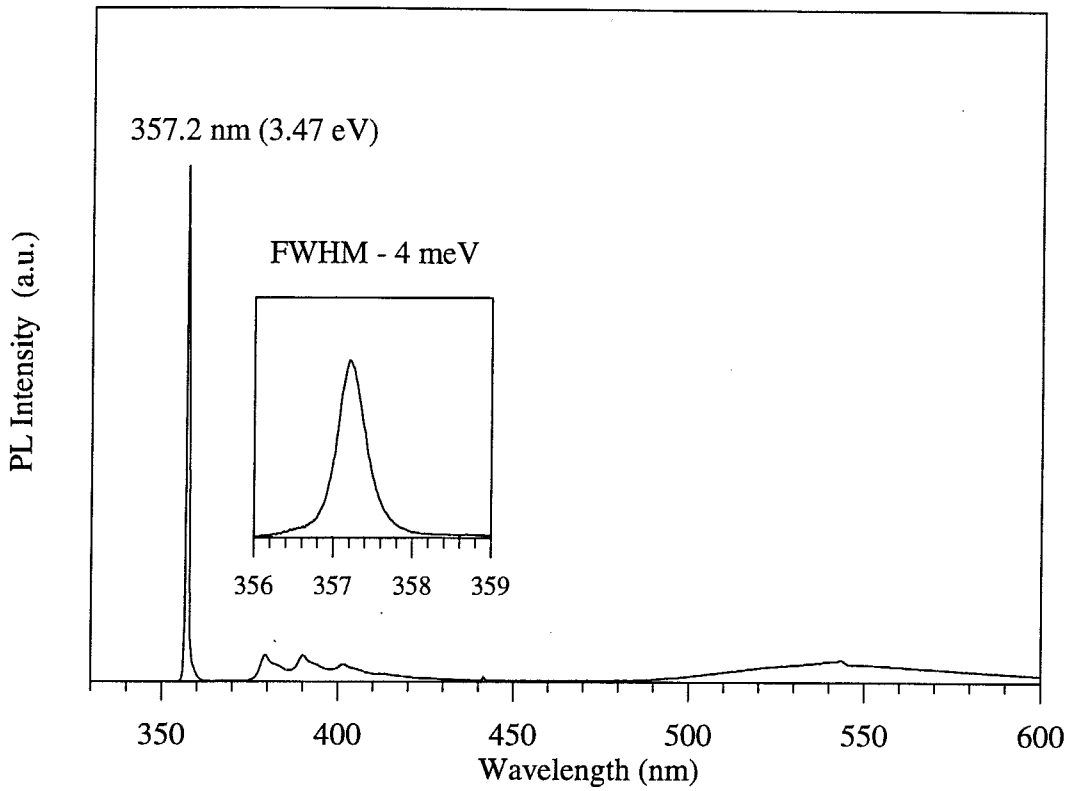

Figure 3. PL of undoped GaN at 8K.

donor-acceptor (DA) defect peaks were relatively weak in this sample, as was the deep level (DL) emission at 540 nm.

The effect of growth temperature on the photoluminescence of GaN is shown in Fig. 4. All three samples were .6-.7 μm thick. At the higher growth temperatures the DA peaks increased in intensity relative to the band-edge emission. The sample grown at 900 °C exhibited the best luminescence. Subsequent tests showed that 950 °C was the optimal growth temperature, as judged by electrical, microstructural, and structural characterization. Modifications of the growth parameters improved the PL as well (Fig. 3).

The PL of Si-doped GaN is shown in Fig. 5, as a function of carrier concentration. The two main peaks in the spectrum are the band edge emission at 358 nm and the DL peak at 540 nm. The peak at the band edge broadened and moved to lower wavelengths as the doping level was increased, with the peak wavelengths at 358.3 nm, 358.24 and 358.0 for the three samples. This is typical behavior for n-type semiconductors. It is believed that the band-edge peak is due to donor to valance band transitions, but lower carrier concentrations are needed to verify this. The deep level emission at 540 nm also increased in intensity as the doping level increased.

The PL of Mg-doped GaN exhibited blue emission, as shown in Fig. 5. These results proved to be repeatable. This sample was annealed in flowing N_2 for 90 minutes at 800 °C.

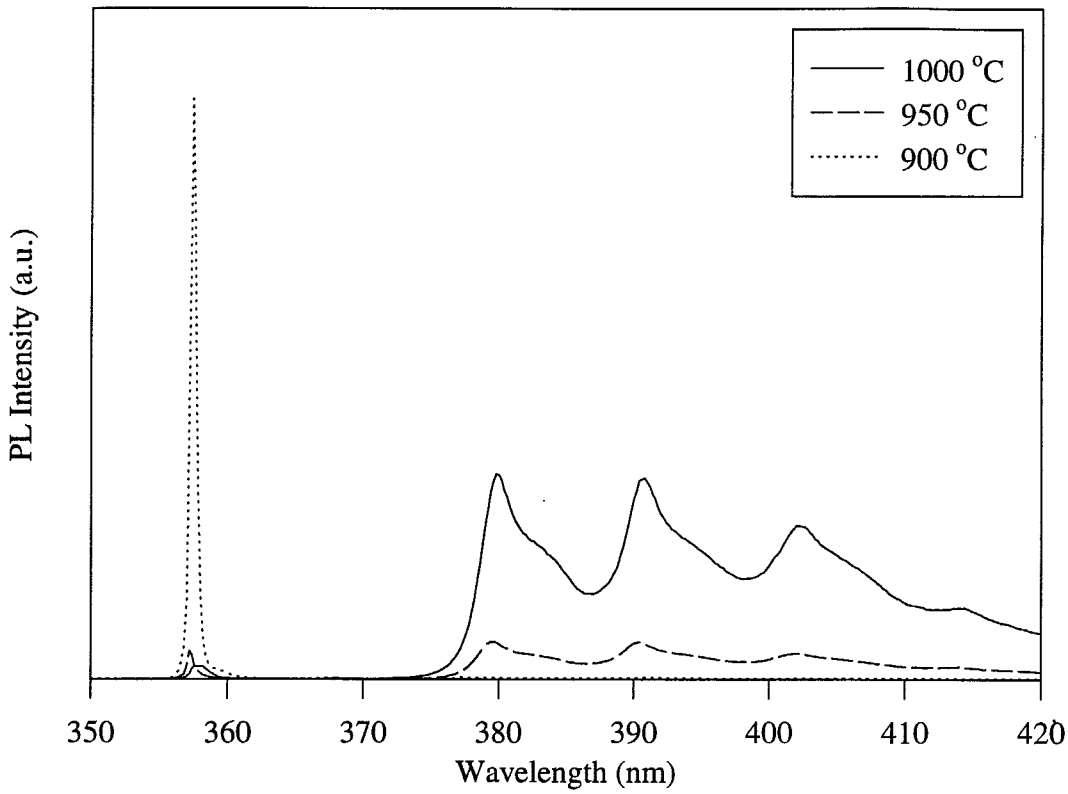

Figure 4. PL of GaN as a function of growth temperature.

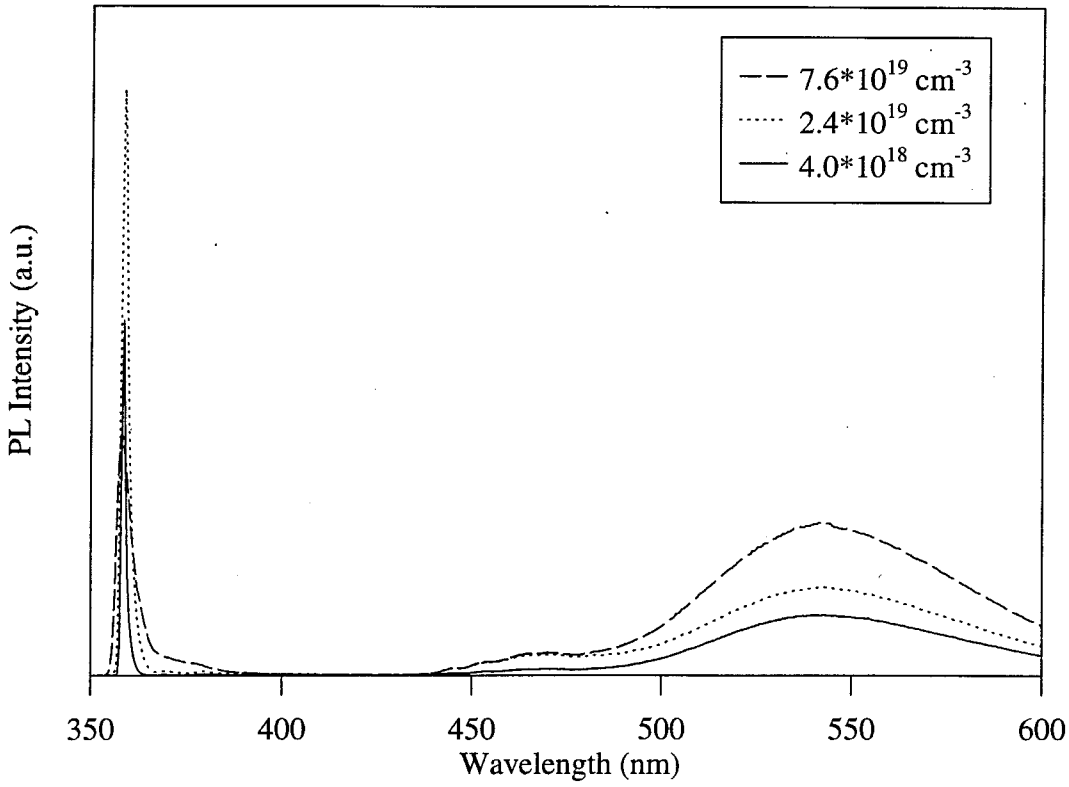

Figure 5. PL of GaN as a function of growth temperature.

The peak wavelength of 426 nm was typical for the samples tested. PL performed at room temperature showed that the samples exhibited blue emission at a lower intensity.

Cathodoluminescence was performed on two $Al_xGa_{1-x}N$ samples, and the results are shown in Fig. 6. Each sample was doped with silicon. The results indicate that near band-edge emission was obtained for both samples. Further tests are needed to better understand the origin of the deep emissions seen in each sample.

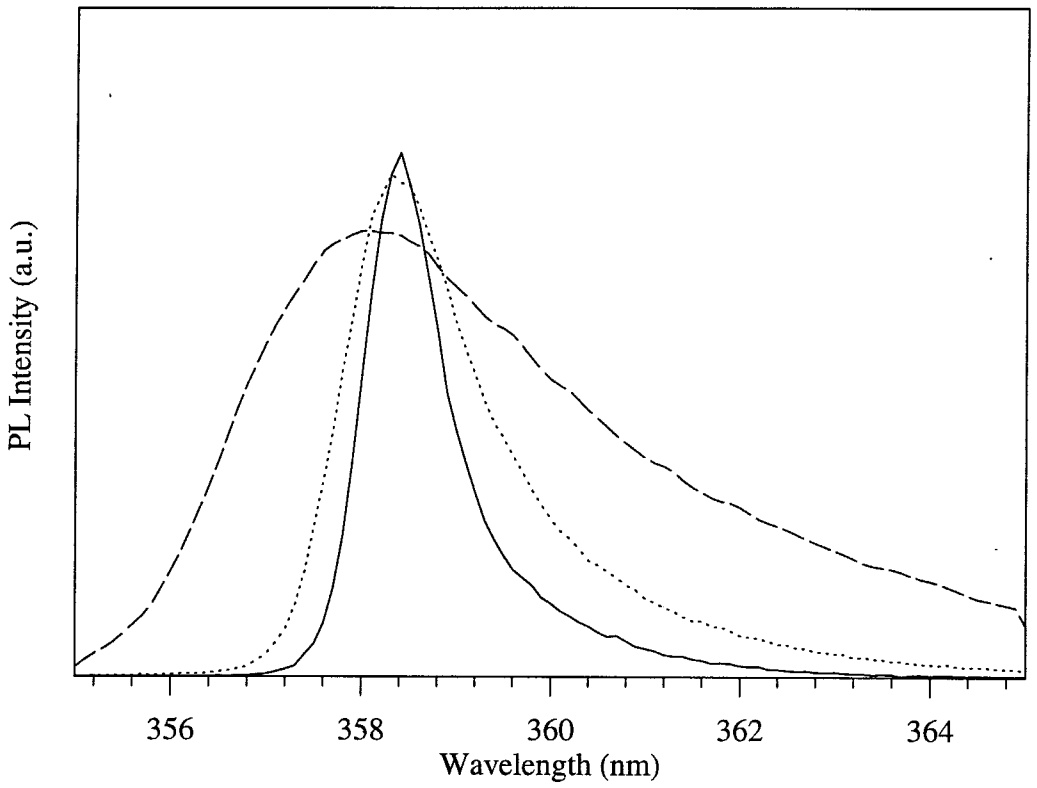

Figure 6. PL of GaN as a function of growth temperature.

D. Conclusions

Low temperature (8K) photoluminescence has been used to characterize both undoped and doped GaN films deposited on vicinal α(6H)-SiC(0001)$_{Si}$ wafers by OMVPE. Unintentionally doped GaN exhibited a sharp peak at 357.2 nm that is due to the recombination of excitons at neutral donors. The FWHM of 4 meV of the peak is an indication of the high quality of the films. The film thicknesses for the results reported were all below 1 μm, which indicates that thicker films are not required to improve the PL data.

The PL of Si-doped GaN showed two peaks that dominate the spectrum, a near-band edge peak at 358 nm which is probably due to donor to valance band transitions, and a peak at 540 nm due to DL emission. As the carrier concentration increased the band-edge peak

broadened and moved to higher energies, while the DL peak increased in intensity. Mg-doped GaN exhibited a broad blue spectrum that peaked at 426 nm. These samples were annealed in flowing N_2 for 90 minutes at 800 °C.

Cathodoluminescence was used to characterize two Si-doped $Al_xGa_{1-x}N$ films. The results indicate that CL is a useful tool for analyzing films which have a band gap higher than that which can be tested by the He-Cd laser. In the future the CL of both undoped and doped $Al_xGa_{1-x}N$ films will also be performed to measure their quality.

E. Future Research Plans and Goals

Photoluminescence and cathodoluminescence will continue to be used to measure the quality of GaN films grown by OMVPE. CL measurements of $Al_xGa_{1-x}N$ films through the full composition range will also be performed. In addition, PL will be used to guide the growth of $In_xGa_{1-x}N$. A new GaAs photomultiplier tube (PMT) with a wavelength range of 180-930 nm will be added to the system to assist in this. This PMT will also make it possible to measure deep levels that occur in Mg-doped GaN, which have been found in samples that were not fully annealed.[5]

The present system will be improved by placing the monochrometer on an optical table. This will allow for a variety of experiments outside of the sample chamber shown in Fig. 1. One application will be to measure the spectral output, external quantum efficiency, and total output power of LEDs with the aid of an integrating sphere. PL measurements will also be made using the breadboard.

Future collaboration include working with Dr. J. J. Song at Oklahoma State on photopumping and time-decay studies of $Al_xGa_{1-x}N$ and $In_xGa_{1-x}N$. Deep level transient spectroscopy (DLTS) measurements will be made with the assistance of Dr. Nobel Johnson at Xerox PARC. A collaboration with Dr. Barbara Goldenberg of Honeywell will study the photoluminescence of AlN and $Al_xGa_{1-x}N$ using an ArF excimer laser.

F. References

1. B. G. Yacobi and D.B. Holt, Cathodoluminescence Microscopy of Inorganic Solids, Plenum Press, New York (1990).
2. Micheal D. Lumb, Ed., Luminescence Scpectroscopy, Academic Press, New York (1978).
3. S. Strite and H. Morkoç, J. Vac. Sci. Technol. B, **10** (4) 1237-1266 (1992).
4. R. A. Youngman and J. H. Harris, J. Am. Ceram. Soc., **73** [11] 3238-46 (1990).
5. S. Nakamura, T. Mukai, and M. Senoh, Jpn. J. Appl. Phys., **30** (10A) 1708-1711 (1991).
6. V. F. Veselov, A. V. Dobrynin, G. A. Naida, P. A. Pundur, E. A. Slotensietse, and E. B. Sokolov, Inorganic Materials, **25** (9) 1250-4 (1989).
7. J. N. Kuznia, M. A. Kahn, D. T. Olson, R. Haplan, and J. Freitas, J. Appl. Phys. **73** (9) 4700-4702 (1993).
8. H. Murakami, T. Asahi, H. Amano, K. Hiramatsu, N. Sawaki, and I. Akasaki, J.Crystal Growth, **115** 648-51 (1991).

9. K. Maier, J. Schneider, I. Akasaki, and H. Amano, Jpn. J. Appl. Phys., **32** (6) 846-848 (1993).
10. I. Akasaki, and H. Amano, J. Crystal Growth, **99** 375-80 (1990).
11. S. Yoshida, H. Okumura, S. Misawa, and E. Sakuma, Surf. Sci., **267** (7) 50-53 (1992).
12. S. Nakamura, T. Mukai, and M. Senoh, Jpn. J. Appl. Phys., **31** (9) 2883-90 (1992).
13. S. Nakamura, N. Iwasa, T. Mukai, and M. Senoh, Jpn. J. Appl. Phys., **31** (5) 107-15 (1992).
14. S. Nakamura, T. Mukai, and M. Senoh, Jpn. J. Appl. Phys., **30** (12A) 1998-2001 (1991).
15. S. Strite, J. Ruan, Z. Li, N Manning, A. Salvador, H. Chen, D. J. Smith, W. J. Choyke, and H. Morkoç, J. Va. Sci. Technol. B **9** (4) 1924-29 (1991).
16. W. J. Choyke and I. Linkov, Inst. Phys. Conf. Ser., **137** 141-147 (1993).
17. S. Pacesova and L. Jastrabik, 1979 Phys. Stat. Sol. B **93** K111.
18. S. Yoshida, S. Misowa, Y. Fujii, S. Takada, H. Hayakawa, S. Gonda, A. and Itoh, J. Vac. Sci. Technol., **16** (4) 990-3 (1979).
19. E. R. Glaser, T. A. Kennedy, H. C. Crookham, J. A. Freitas, Jr., M. Asif Khan, D.T. Olson, and J. N. Kuznia, Appl. Phys. Lett. **63** (19) 2673-2675 (1993).
20. E. R. Glaser, T. A. Kennedy, J. A. Freitas, Jr., M. Asif Khan, D. T. Olson, and J. N. Kuznia, Inst. Phys. Conf. Ser., **137** (1993).
21. T. Sasaki, T. Matsuoka, A. Katsui, Appl. Surf. Sci. **41/42** 504-508 (1989).

V. Contact Formation to n-type and p-type GaN

A. Introduction

The formation of ohmic contacts with semiconductor materials and devices is a fundamental component of solid state device architecture. As device size has diminished and the scale of integration has increased, the quality of these interfaces has become an increasingly important concern. In addition, the presence of parasitic resistances and capacitances, such as those existing at contact interfaces, becomes more detrimental at higher operating powers and higher oscillation frequencies. For many devices, the losses that occur at the contact interfaces account for a large fraction of the total losses, and as such are responsible for significant impact on device performance.

The development of adequate and reliable ohmic contacts to the compound semiconductors, particularly those with wider band gaps, has met a number of challenges. The subject of ohmic contacts to p- and n-type III-V compounds, mostly GaAs, AlGaAs, and InP, has received a great deal of attention over the past decade, and significant advances have been made [1-12]. By comparison, the III-V nitrides have received little attention in this regard. However, interest in these materials has been renewed in recent years as thin film growth techniques have improved, p-type doping in GaN and AlGaN solid solutions has been achieved, and p-n junctions have been fabricated.

The majority of successful ohmic contact systems that have so far been implemented with the more conventional compound semiconductors have relied upon alloying (liquid-phase reaction) or sintering (solid-phase reaction) via post-deposition annealing treatments, and/or the presence of high carrier concentrations near the interface [1,2,6,12]. However, many otherwise successful ohmic contact systems have only limited thermal stability and are subject to degradation, usually in the form of extensive interdiffusion, interfacial reaction, and interphase growth, accompanied by increase in contact resistivity, under subsequent thermal processing steps. It is reasonable to suppose that the cleanliness and preparation of the semiconductor surface prior to contact deposition plays a significant role in the behavior of the interface, and there are indications in the recent literature that support this [2,11-13]. Thorough oxide removal is especially important, though it may well prove to be a persistent challenge with Al-containing compounds in particular.

In this study, two main approaches are being taken in the development of ohmic contacts to GaN and AlN. The first approach is similar to that which has resulted in the majority of successful ohmic contacts to the more conventional compound semiconductors such as GaAs: the creation of high carrier concentrations in the semiconductor at the metal interface by means of alloying, sintering, or implantation of dopant species. The so-called pinning of the Fermi level at this surface, particularly with GaAs, results in a more or less fixed potential barrier at

the metal interface. In the case of the pinned Fermi level of GaAs, the approach has generally been to shrink the width of the depletion layer by means of increasing the carrier concentration to the point where carrier tunneling through the barrier occurs readily. Even with optimization of contact composition and annealing times and temperatures, the lowest contact resistivities (ρ_c) have been obtained only on the most heavily doped materials. Though there are indications that high doping levels and extensive interfacial reactions through alloying and sintering are not essential for ohmic contact formation in all cases, these processes have proven useful for minimizing ρ_c [2,11-13].

The other approach toward ohmic contact formation to be taken in this study involves the Schottky-Mott-Bardeen (SMB) model of semiconductor interfaces [14,15]. In this model the relative values of work function of the materials involved determine the band structure of the interface and thus the nature of any potential barriers present. The presence of interfacial states at the semiconductor surface can interfere with the alignment of the Fermi level across the interface and overshadow the effect of the inherent difference in work function between the two materials. The III-V nitride compounds are more ionically bonded than their phosphide and arsenide counterparts, as a result of larger electronegativity differences between the component elements. According to the observations of Kurtin *et al.* [16], this fact indicates that the nitrides should experience less Fermi level stabilization or "pinning" at the surface than do the more covalent compounds. Thus, the barrier heights of contacts to the nitrides should be more dependent on the contact material than is the case with the more conventional and more covalent semiconductors such as Si, GaAs, InP, SiC, etc. With the work of Foresi and Moustakas [17,18], this concept is beginning to be investigated. The SMB model also indicates that the cleanliness of the interface plays an important role in its electrical behavior, particularly in the minimization or elimination of any insulating layers at the interface.

To date, several alloyed and sintered contact strategies, having demonstrated effectiveness with GaAs - and, in the case of Au, with GaN - have been undertaken with GaN and AlN. The tighter bonding of Ga and Al to N, in comparison to As, suggests that higher temperatures and possibly longer times are required for interfacial reactions to take place, and that some reactions may be inhibited or prevented. The behavior of the systems examined so far has been consistent with these suppositions. Contact strategies involving the concentration of active dopant species at the contact interface will continue to be characterized in this study, as well as the investigation of the roles of work function differences and interfacial cleanliness. In the present reporting period, both of these approaches to contact formation were continued.

One area of contacts development that has received a significant amount of attention is that of the metal silicide compounds. Silicide thin films have been extensively studied and applied as contacts and interconnects, mostly for silicon-based technology [19-24]. In comparison, the properties of the metal germanides are not well documented. As a general rule, germanides

have been found to be more resistive than silicides and their chemistry with Si-based materials more complex. However, in a series of studies, M. O. Aboelfotoh *et al.* have shown that a particular phase of copper germanide, specifically the ordered monoclinic phase ε_1-Cu_3Ge, is an exception to these rules [25-28]. Thin films of Cu_3Ge exhibit remarkably low resistivities, unlike Cu_3Si, and, unlike both Cu and Cu_3Si, are surprisingly stable with respect to oxygen and air exposure. As such, Cu_3Ge presents itself as a potentially useful contact metal. Indeed, preliminary experimentation with Cu_3Ge contacts on GaAs and GaN, primarily on n-type and heavily-doped p-type material, has produced some favorable results in terms of ohmic contact formation. For these reasons copper-germanium contacts were investigated during this reporting period as possible candidates for high-quality, low-resistivity ohmic contacts.

B. Experimental Procedure

Film Deposition. The substrates used for III-nitride film growth were 6H-SiC wafers supplied by Cree Research, Inc. Two growth methods have been used for the deposition of III-N films for these contacts studies: ECR plasma-enhanced molecular beam epitaxy (MBE) and metalorganic vapor phase epitaxy (MOVPE). The growth reactors used for the nitride film deposition are described in other sections of this report. Magnesium incorporated into the films during growth as the p-type dopant; Ge was used to grow n-type material via MBE and Si was used as the more effective donor impurity for the MOVPE-grown films.

Six different contact systems were examined during this reporting period. Contacts deposited on n-GaN (Si or Ge-doped) were: (1) single Al layers, (2) an alloyed compound of Cu_3Ge, and (3) TiN layers. The contacts deposited on Mg-doped GaN were: (1) single Au layers, (2) single Pt layers, and (3) a Au/Mg/Au multilayer contact. Prior to metals deposition, the nitride films were cleaned with a 50:50 $HCl:H_2O$ dip and carefully pulled dry from the solution. Any remaining cleaning solution was blown dry with N_2. A shadow mask was used during deposition to create rectangular-bar TLM (transmission line model) patterns for contact resistivity (ρ_c) measurements, as described in the earlier semiannual report of June 1993. The variety of contact metals used in this study has necessitated the use of different deposition systems with differing capabilities. The Au layers, Cu/Ge layers, and Au/Mg/Au layers were deposited by means of electron beam evaporation using a Thermionics evaporation system having a 3 kW 5-source electron gun. The 5-source capacity of the e^--beam hearth allowed the deposition of multiple layers of different metals in the same vacuum run. Film thicknesses were monitored using a quartz crystal oscillator. The Al layers were deposited in a standard thermal evaporator, while the much more refractory Pt films were deposited by means of Ar ion sputtering. Lastly, the TiN films were grown by means of ion-beam assisted deposition (IBAD) in a UHV electron-beam evaporation system containing a Kaufman-type ion source for N_2 activation.

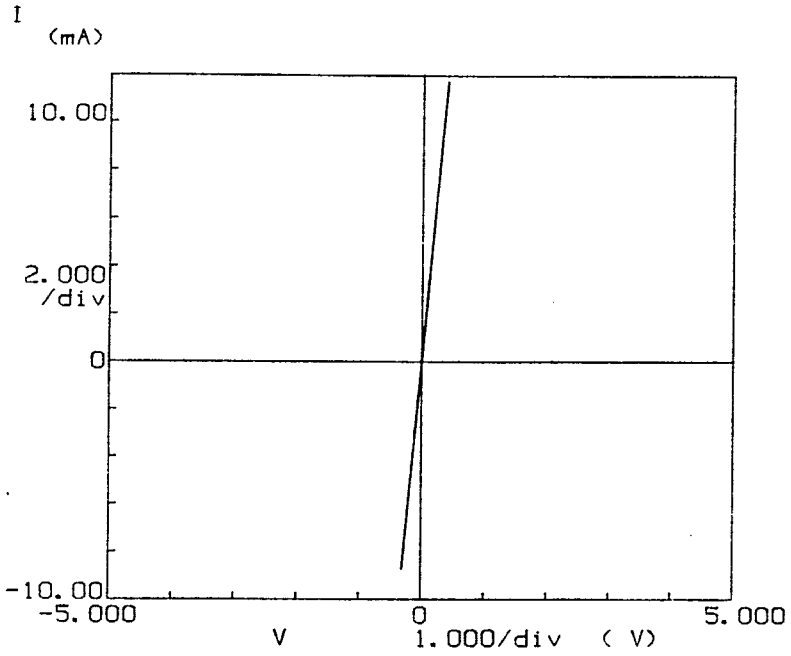

Figure 1. I-V data for as-deposited Al contacts on n-type GaN.

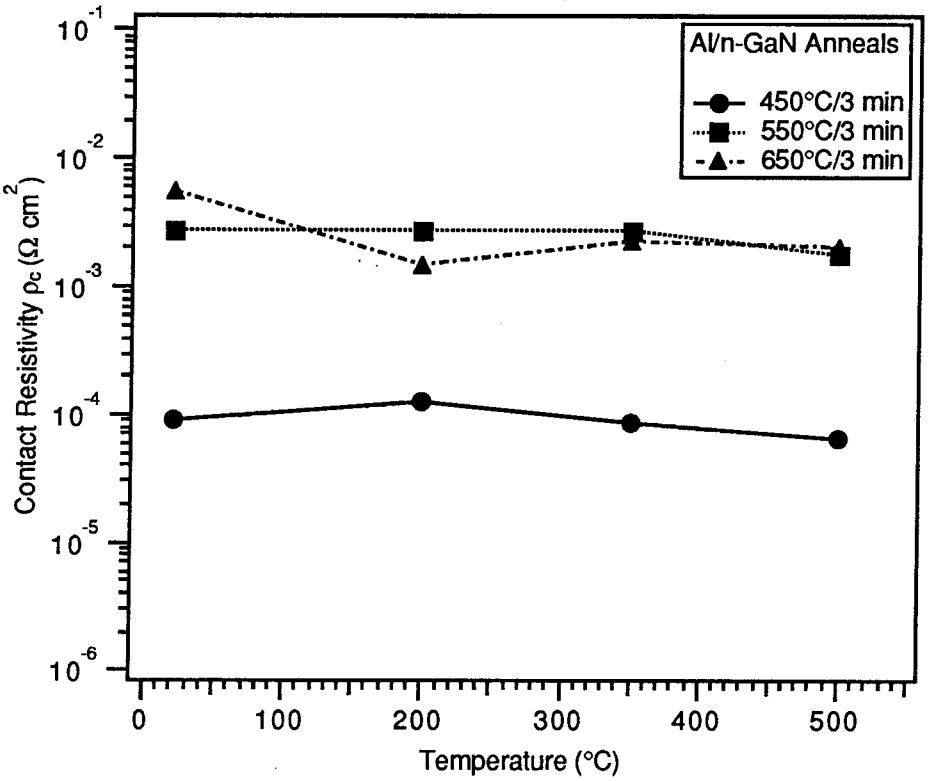

Figure 2. Contact resistivities of Al /Ge:GaN as a function of measurement temperature and heat treatment.

condition, the measured resistances and contact resistivities decreased slightly with increasing temperature due to the greater thermal availability of free charge carriers. After annealing at 450°C, the behavior of the Al contacts was essentially unchanged from the as-deposited condition. However, the 550°C and 650°C anneals resulted in an overall increase of contact resistivity, even with the reduced resistances that occurred at higher measurement temperatures. After annealing to 650°C, the contact resistivity stabilized at approximately 2×10^{-3} Ω cm^2.

Characterization by means of cross-sectional TEM (X-TEM) is being performed on the contact systems in this study by our collaborators at Arizona State University to investigate the interfacial structures in detail. The Al film as initially deposited was polycrystalline with somewhat columnar growth, oriented randomly with respect to the GaN surface. Annealing resulted in grain growth in the Al layer, but no change in the random orientation with respect to the GaN lattice. In addition, this analysis of the Al/n-GaN contact interface shows that a new phase formed at the Al/GaN interface as a result of heat treatment. Cross-sectional TEM images of the Al/GaN interface, annealed at 650°C for 3 min, are shown in Fig. 3. The appearance of this interfacial phase as a result of annealing correlates with an increase in contact resistivity, which suggests the formation of higher-resistivity materials at the interface and thus may indicate the presence of an Al nitride phase. Selected-area diffraction analysis (SAD) of these second phase regions indicates a cubic structure with a lattice parameter of 7.84 Å. These second phase particles at the interface, which do not form a continuous layer, range in size from about 50-800 Å; smaller particles of the same phase were found farther into the Al layer, about 10-100 Å in size. Spectroscopic analysis via EELS revealed the presence of nitrogen in the Al layer, but no appreciable amounts of Ga. Some oxygen was also found in the Al layer, though at this time it is not clear how much of this oxygen originated at the sample surfaces and how much of it was incorporated in to the Al film during thermal evaporation in a non-UHV environment.

Cu_3Ge Contacts on Ge:GaN. The Cu_3Ge contacts on n-type GaN (MBE, Ge-doped) were deposited at IBM's Yorktown Heights research facility in a UHV e$^-$-beam evaporation system. The Cu and Ge components of this contact system were deposited sequentially, 800 Å layers of Cu followed by 1200 Å of Ge; the alloying of the layers was accomplished by heating at 400°C for 15 minutes, while in vacuum after the metal evaporation, as described by Aboelfotoh *et al.* [25-28]. Current-voltage data for Cu_3Ge contacts on Ge-doped GaN, shown in Fig. 4, reveal ohmic behavior with low overall resistance. In addition, the contacts retained a shiny, smooth surface, indicative of little or no roughening or reaction at the interface. This good contact behavior contrasts with the results reported in the last semi-annual report for this project (June 1994), in which the Cu/Ge layers were sequentially deposited in a non-UHV, bell jar-type evaporation system and alloyed at 1 atm (N_2) in an RTA furnace. Subsequent SIMS analysis of these earlier, non-UHV-deposited Cu_3Ge films revealed a substantial presence of

oxygen in the metal. These observations indicate that the deposition and alloying environment plays an important role in the character and performance of the electrical contacts that form. Further characterization of the Cu_3Ge contact system, including TLM measurements and microstructural analysis, will be performed in the coming weeks.

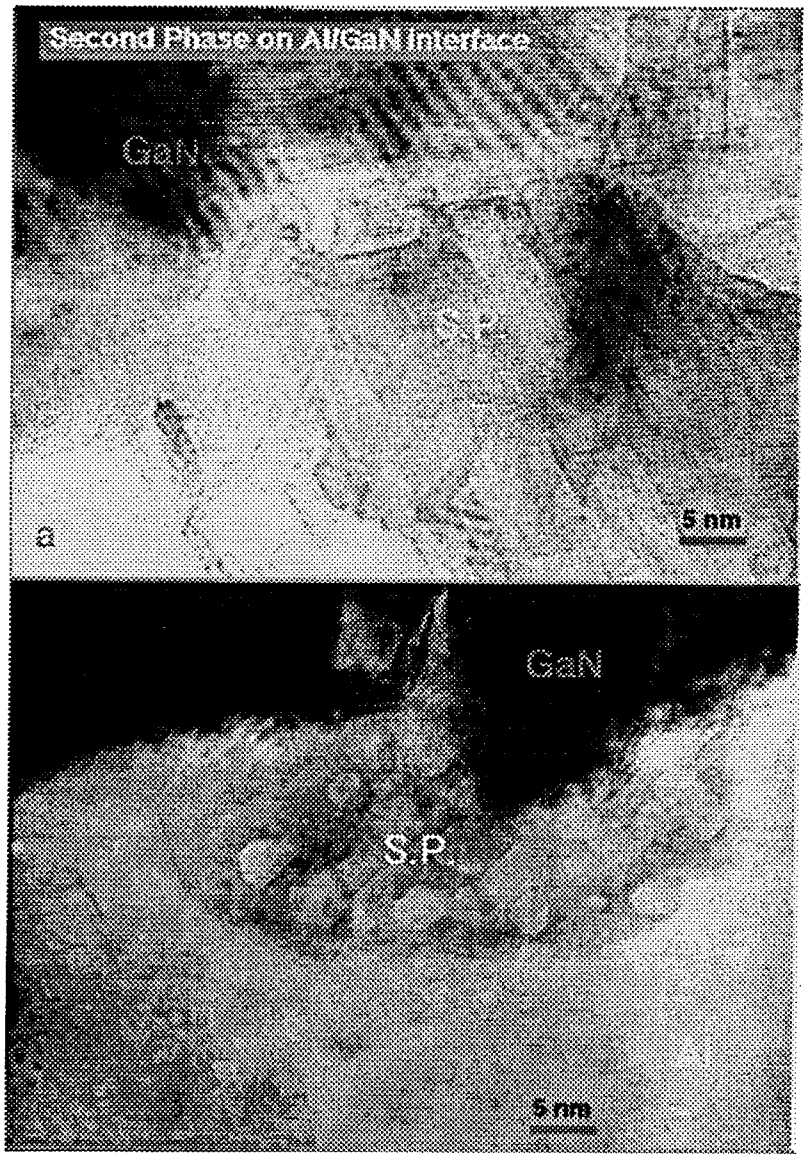

Figure 3. High-resolution X-TEM images of Al /GaN interface, annealed at 650°C for 3 min. Both images, taken at the same magnification in two different regions of the interface, show a new crystalline phase forming at the Al/GaN interface.

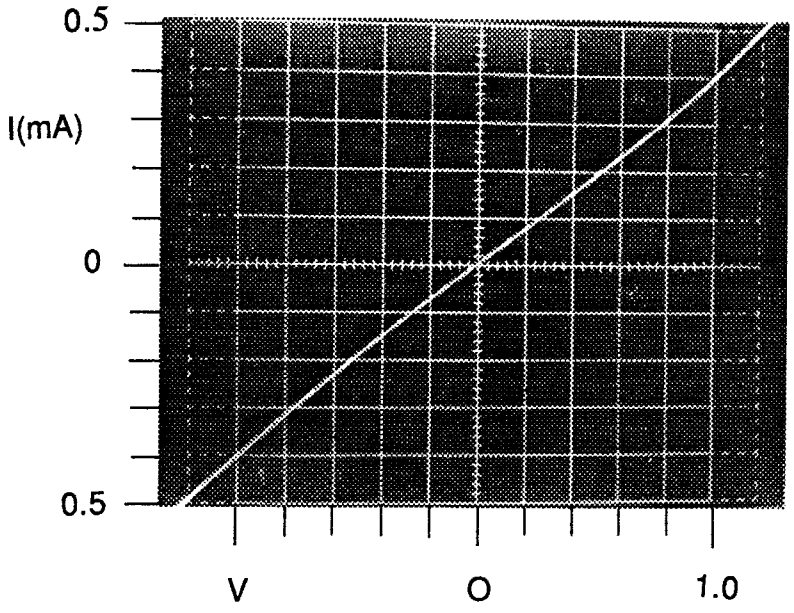

Figure 4. I-V data for as-alloyed Cu_3Ge contacts on Ge-doped GaN.

TiN Contacts on Si:GaN. Titanium nitride was grown on Si-doped GaN (MOVPE-grown) by means of ion beam-assisted deposition (IBAD), using e⁻-beam evaporation of Ti and purified N_2 activated by a Kaufman-type ion gun. The TiN growth was performed at a substrate temperature of 350°C and a deposition rate of 10-15 Å/min. Auger depth-profiling analysis of films grown under these conditions have revealed them to be stoichiometric TiN and uniform through the thickness even when variations in pressure and deposition rate occurred during growth. In addition, the metallic gold-like appearance of the TiN compound is a reliable indicator of stoichiometry.

Current-voltage measurements of TiN/n-GaN contacts, shown in Fig. 5, reveal them to be linearly ohmic in the as-deposited condition. TLM measurements of this contact system yield a very low specific contact resistivity at room temperature, estimated to be in the low 10^{-7} Ω cm² range; the lower limit of ρ_c measurement has been discussed above in the Experimental Procedure section. Elevated-temperature TLM measurements showed that the ρ_c increased with increasing temperature, into the 10^{-3} Ω cm² range, and returned to its room-temperature behavior after cooling.

Au contacts on Mg:GaN. The preliminary electrical characterization of Au contacts on p-type Mg:GaN was described in last year's annual report for this project (December 1993). These Au/p-GaN contacts were rectifying as-deposited, though not close to being ideal Schottky contacts, and were found to yield linearly ohmic I-V behavior after annealing at sufficiently high temperatures (>650°C). Annealing at 800°C for 10 minutes, after earlier

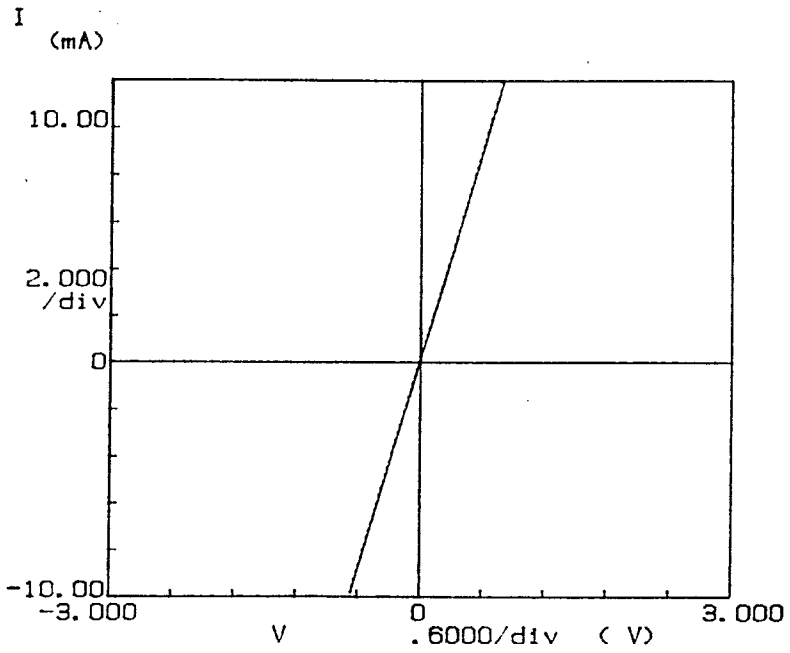

Figure 5. I-V data for as-deposited TiN contacts on Si-doped GaN.

anneals at lower temperatures, resulted in a ρ_c drop of over 3 orders of magnitude into the $10^1\ \Omega\ cm^2$ range. This change in contact behavior, shown in Fig. 6, was associated with some visible roughening of the Au surface, indicative of interfacial roughening, and noticeable inter-mixing of the metallic elements at the interface was observed in Auger depth-profiling analysis.

Cross-sectional microstructural characterization has since been performed on this contact system by means of X-TEM, and high-resolution images reveal that interfacial reaction did indeed occur as a result of annealing at high temperature. In addition, during the preparation of TEM specimens, it was observed that there was poor adhesion of the Au to the GaN surface in both the as-deposited and annealed conditions. Figure 7 shows the formation of an amorphous phase at the annealed Au-GaN interface, extending into the apparently decomposing GaN lattice. Some cavities were also seen at the interface, which almost certainly contribute to the poor adhesion. Spectroscopic analysis by means of EELS revealed the presence of nitrogen throughout the Au layer; compositional characterization of the amorphous regions is currently underway. The Au layer (2500 Å thick) was polycrystalline as-deposited, and while grain growth in the Au film occurred during annealing, no particular crystallographic orientation or relationship was observed between the Au and the GaN.

Au/Mg/Au contacts on Mg:GaN. A three-layer Au/Mg/Au (320 Å/320 Å/1700 Å overlayer on top) contact system was deposited on Mg-doped GaN by means of e$^-$-beam evaporation. In contrast to the Au single-layer contacts, the Au/Mg/Au contacts with only

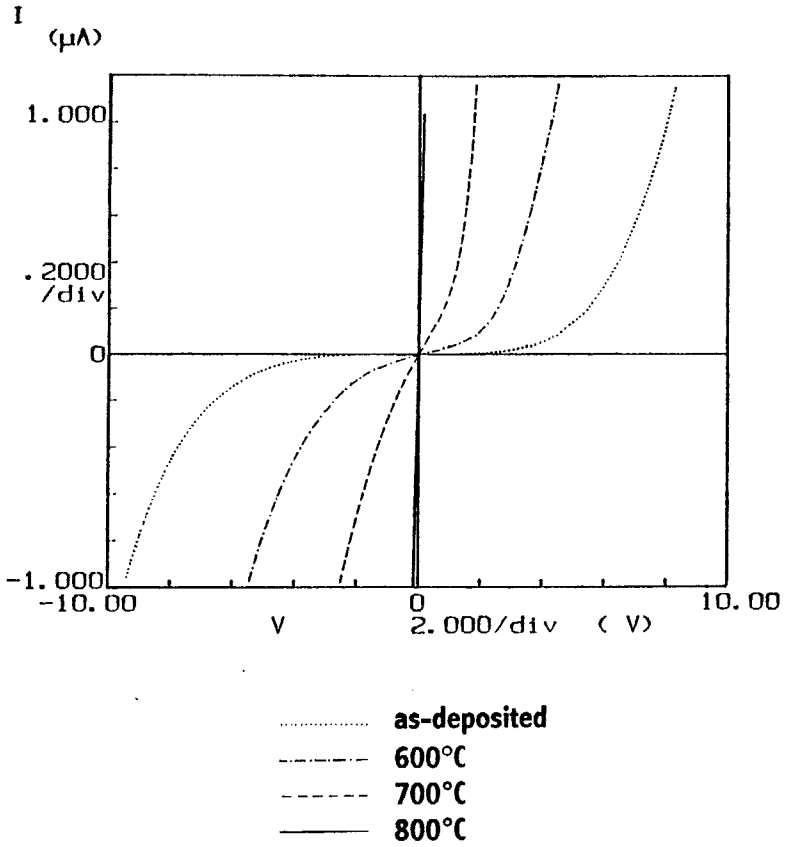

Figure 6. I-V behavior of Au/Mg:GaN contacts as a function of annealing temperature, showing transition to ohmic behavior.

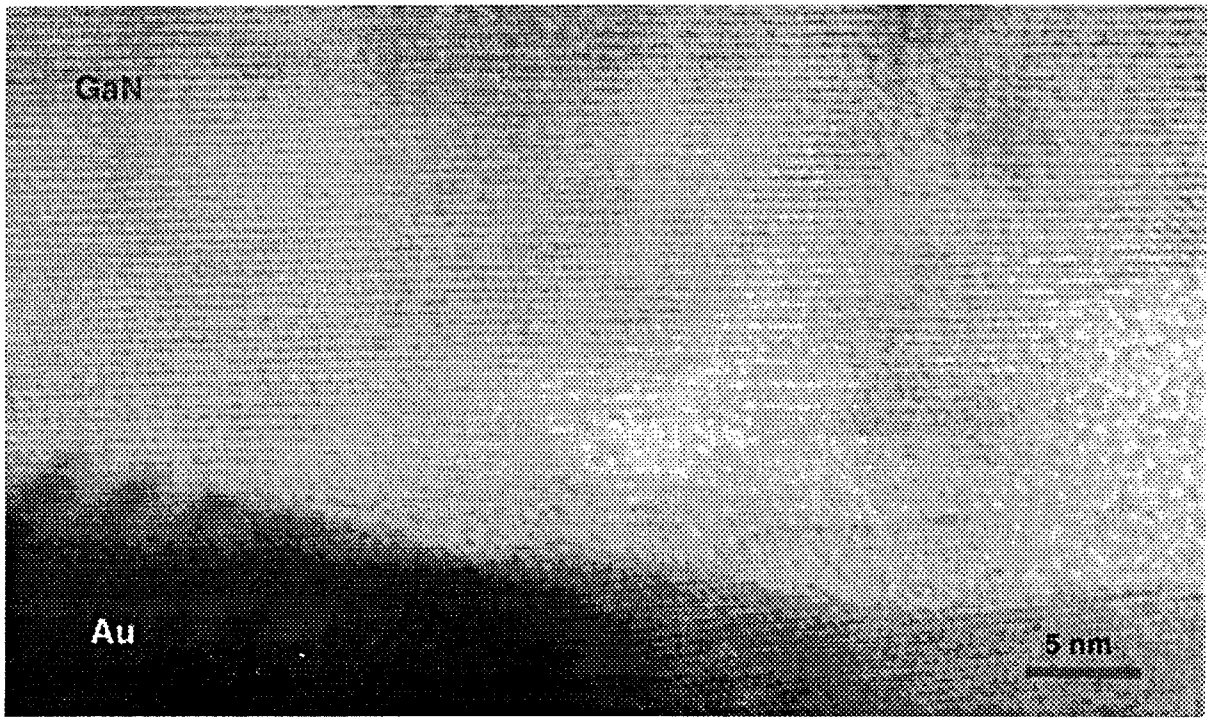

Figure 7. High-resolution X-TEM image of Au/GaN interface, annealed at 800°C for 10 min, showing formation of amorphous phase as a result of high-temperature annealing.

320 Å in direct contact with the GaN surface, followed by the Mg layer, were linearly ohmic in the as-deposited condition; this is shown in Fig. 8 below. Contact resistivity measurements yielded a room-temperature ρ_c of 214 Ω cm^2. Figure 9 shows the results of elevated-temperature ρ_c measurements. The ρ_c dropped off substantially at elevated temperatures, down to 2.7×10^{-1} Ω cm^2 when measured at 350°C. This behavior remained essentially unchanged after heat treatments of 575°C and 650°C, for 15 s each. After a further annealing treatment at 725°C for 15 s, the contacts became substantially more resistive. Cross-sectional microstructural characterization of this contact system, both as-deposited and annealed, is currently underway.

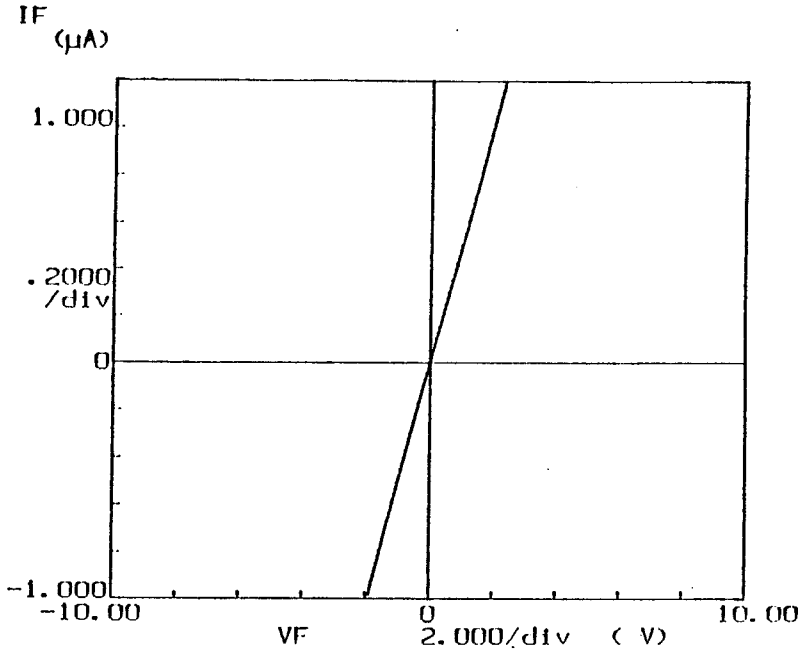

Figure 8. I-V data for as-deposited Au/Mg/Au contacts on Mg-doped GaN.

Pt Contacts on Mg:GaN. Pt contacts were deposited on Mg-doped GaN by means of Ar-ion sputtering. There was no deposition thickness monitor in the sputtering system, but from reported deposition rates the Pt film thickness is estimated to be 500-600 Å. These contacts were found to be ohmic as-deposited, as shown in Fig. 10 below, and to have a ρ_c that is evidently substantially lower than the range of precise calculation, which means much less than 10^{-6} Ω cm^2. When measured at elevated temperatures up through 400°C, this behavior remained throughout well below the range in which it could be calculated. These initial results are very promising and demand further confirmation and more precise characterization. Annealing studies of this contact system, as well as further depositions, will be performed in the coming weeks. Microstructural characterization is also upcoming in the very near future.

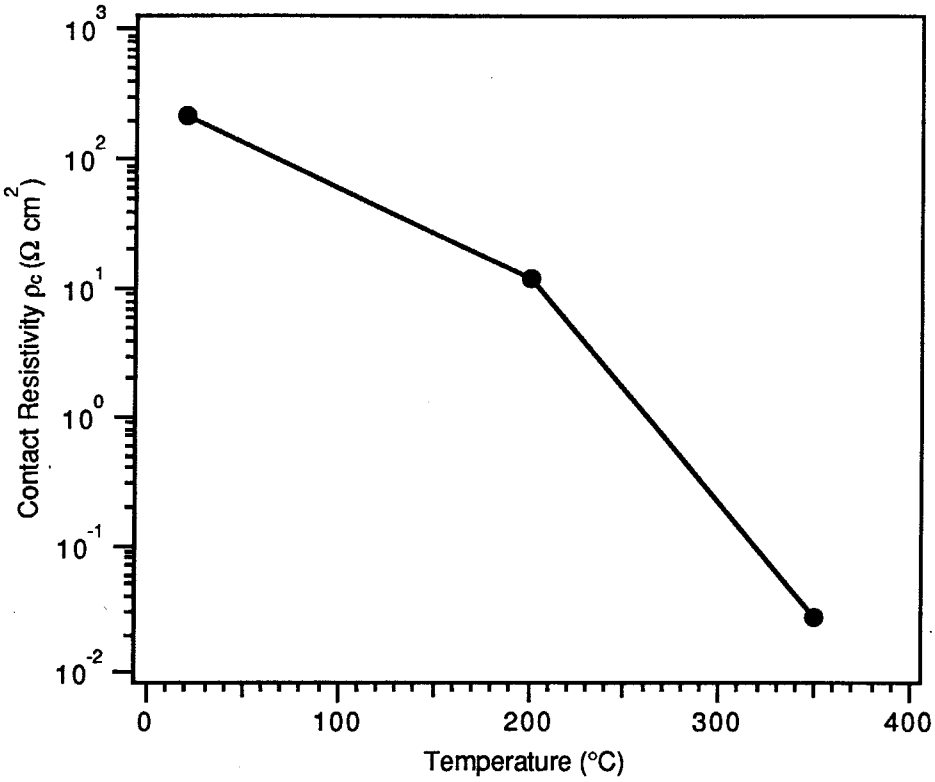

Figure 9. Contact resistivities of Au/Mg/Au/p-GaN system as a function of temperature.

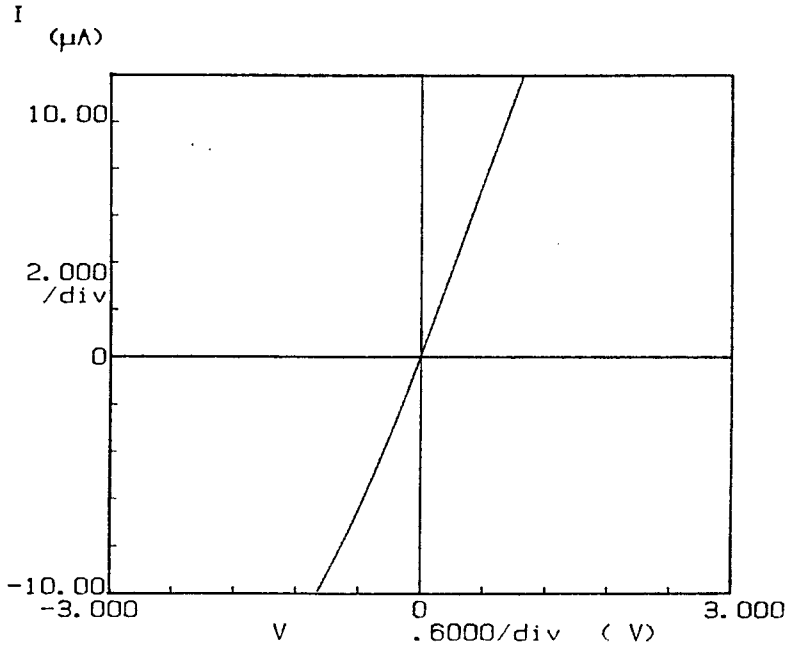

Figure 10. I-V data for as-deposited Pt contacts on Mg-doped GaN.

D. Discussion

Al Contacts on Ge:GaN. That the as-deposited Al contacts on Ge-doped GaN would prove to be ohmic is consistent with the Schottky-Mott-Bardeen model, based on the relationship of the work functions of the two surfaces. Aluminum is a relatively low work function metal (ϕ_{Al}=4.2 eV) and thus provides a favorable band offset for ohmic contact formation to an n-type semiconductor (ϕ_{GaN} estimated to be 4.1 eV). However, it should be pointed out that the exact value for the work function and/or electron affinity of GaN and their dependence upon doping levels have not been reproducibly and precisely established as yet. As stated above, the results of these contact resistivity measurements compare very favorably with those reported by Foresi and Moustakas [17,18], and, more recently, Lin *et al.* [30]. The GaN materials used by both of these groups were different than those used in this study; theirs were unintentionally doped and inherently n-type, indicative of high background carrier concentrations (about 10^{17} cm^{-3} in both cases) and defect densities. Hall measurements of Ge:GaN films similar to those used for contact deposition and TLM measurements in this study yielded carrier concentrations of about $3x10^{19}$ cm^{-3} with mobilities of approximately 100 cm^2 V^{-1} s^{-1}. Given the fact that contact resistivities tend to be strongly affected by bulk and surface carrier concentrations, it is not surprising that these highly doped Ge:GaN films produced low-resistivity contacts. However, contacts need to be made to more lightly doped material as well, and steps can be taken to improve the performance of such contacts, as described above.

The samples were annealed for short periods of time in an RTA furnace under flowing N_2. The purpose of performing the annealing under N_2 at atmospheric pressure for short times was to reduce the likelihood of generating N vacancies which are believed to be shallow donors that contribute to the background carrier concentration. While increasing the background carrier concentration may contribute to greater current transport in the semiconductor and across the contact interface and apparently reduce the ρ_c, in general such behavior would be detrimental to overall electronic properties and device performance. More extensive characterization of the electronic properties of our nitride films is needed to better correlate and understand the relationship between dopant concentration, carrier concentration and mobility, Fermi levels, and contact behavior. Improvements in our measurement capabilities, in terms of both equipment and sample preparation techniques, are underway.

The results of the X-TEM analysis show that an intermediate phase formed at the Al/GaN interface, possibly a form of AlN, as a result of annealing. The correlation of the formation of this interfacial phase with an increase in contact resistivity is suggestive. Aluminum nitride has a very large and negative free energy of formation and thus the reaction is energetically favored where there is sufficient thermal mobility. The presence of nitrogen and the formation of intermediate phase particles within the Al layer indicates that this is very likely occurring.

CuGe Contacts on Ge:GaN. To date, the properties of Cu_3Ge films have been documented by Aboelfotoh *et al.*, but the interfacial properties of CuGe contacts to semiconductor surfaces are only beginning to be investigated. The results of preliminary TLM measurements, reported in the last semi-annual report for this project (June 1994) show that Cu_3Ge, and also Cu contacts in the as-deposited state, form ohmic contacts on both Ge:GaN and Mg:GaN. The results of I-V measurements of UHV-deposited, alloyed-*in situ* Cu_3Ge contacts indicate low-resistivity ohmic behavior. At the present time the work function and electron affinity properties of CuGe compounds have not yet been studied, so it is not known how this contact system compares with the Schottky-Mott-Bardeen model. It is possible that even if a contact metal does not have a favorable work function relationship to a semiconductor for ohmic contact formation according to the Schottky model, the role of a barrier at the surface can be bypassed by means of other current transport mechanisms. The time intervals and temperatures of the alloying and/or contact annealing steps, along with the cleanliness of the deposition environment, have significant effects on the resulting current-carrying abilities of the contacts. The details of the alloying and annealing procedures would influence the rate and amount of any interfacial diffusion that take place and the reactions that occur at the interface. Film composition is also evidently of critical importance in the behavior of this contact system, given the difference between the UHV and non-UHV-deposited contacts. All of these factors have an effect on the behavior of the contacts. Given the success of this contact system with GaAs materials and its promise for the nitrides, investigations will continue.

TiN Contacts on Si:GaN. TiN is a low work function metal (ϕ_{TiN}=3.74 eV), and thus according to the Schottky-Mott-Bardeen model should be likely to form ohmic contacts to n-type semiconductors. It has the NaCl structure and has a reasonably close lattice match to hexagonal GaN (-5.9 %) and AlN (-3.6 %) in the close-packed (111) planes. In earlier work at NCSU it was shown that TiN forms an epitaxial and ohmic contact on n-type 6H-SiC, which has a lattice parameter similar to that of AlN. In addition, TiN is thermally very stable and highly resistant to oxidation, forming only a thin passive oxide film on the surface. Since in the TiN the Ti is already stoichiometrically nitrided and strongly bound to N, the likelihood of detrimental interfacial reaction is virtually eliminated. As such, it is a good contact candidate, and this experiment was performed to test this supposition.

The TiN/n-GaN contacts did indeed turn out to be ohmic and to have low specific contact resistivity in the as-deposited condition. These recent results may provide some insight into the good performance seen from annealed Ti/Al contacts on n-type GaN [30]: given that thermodynamic data suggest that TiN formation is favored, the presence of TiN at the interface of annealed Ti/Al contacts may be responsible in whole or in part for the observed low contact resistivities. Annealing treatments will be conducted on the TiN contact samples in the coming weeks to investigate the thermal stability of the system. The increase in ρ_c with increasing

measurement temperature contrasts with the results observed with Al/n-GaN and Au/Mg/Au/p-GaN contacts. More detailed study of the temperature-dependent ρ_c behavior is planned in order to understand the current transport mechanisms and establish the utility of this contact system for high-temperature device applications. After the annealing study, X-TEM samples of as-deposited and heat-treated contacts will be sent to ASU for high-resolution microstructural characterization to look for epitaxial relationships and any compositional changes that take place.

Au Contacts on Mg:GaN. The rectifying nature of the as-deposited Au contacts on undoped n-GaN was observed by Foresi and Moustakas in their contacts investigation [17,18]. However, the GaN material used by Foresi *et al.* was different than that used in this study; theirs was undoped and inherently n-type, indicative of a high background carrier concentration and defect density. By contrast, the GaN material used in the present study was Mg-doped; Mg:GaN films grown under the same conditions as these have been found to be p-type, with carrier concentrations of 10^{18} cm^{-3} and low mobilities of about 10 cm^2 V^{-1} s^{-1} [32]. According to the Schottky model, Au should form an ohmic contact on p-type GaN and a rectifying contact on n-type material. However, it should be pointed out that the exact value for the work function and/or electron affinity of GaN and their dependence upon doping levels have not been reproducibly and precisely established as yet; Foresi and Moustakas obtained ohmic contacts with Au on undoped n-GaN after annealing at 575°C for 10 minutes in a reducing atmosphere; according to their TLM measurements they achieved contact resistivities in the range $1.6\text{-}3.1\times10^{-3}$ Ω cm^2. In the present study, the contact resistivities obtained from Au on Mg-doped GaN were higher. Also, the samples in this study were annealed for short periods of time in an RTA furnace under flowing N_2. It is possible that more extensive interfacial reaction than seen in this study would occur in a conventional annealing furnace, as used in the other studies, over longer periods of time.

The change in appearance and texture of the Au surface after high-temperature annealing was evidently due to reactions and/or interdiffusion taking place between the Au and GaN. Interfacial reactions with contacts on GaAs typically show a significant amount of interphase formation and roughening of the interface. The roughening of the interface due to reaction and phase formation may help to lower ρ_c by increasing the area of contact between the metal layer(s) and the semiconductor. The lumpiness of the annealed Au film is indicative of metallurgical reaction and phase formation, and the balling-up effect implies a lack of good "wetting" of the GaN surface. The lack of good wetting of the GaN by Au is also indicated by the poor adhesion of Au to GaN, in both the as-deposited state and the annealed state. The results of X-TEM characterization indicate that under thermal activation N diffused out of the GaN and into the Au layer, thereby freeing the Ga to react and possibly form compounds with the Au. Gallium nitride lacks the very mobile As species of GaAs and has stronger interatomic

bonding, but sufficiently high temperatures and favorable chemistry can nevertheless free the Ga and N from one another. The results of elemental analysis of the amorphous interfacial phase should help determine its composition. Amorphous Au-Ga alloys have been observed before in thin-film deposition, that remain amorphous even up to room temperature [33], which may be forming at the Au/Ga interface upon annealing. On the other hand, the presence of holes and cavities in the annealed Au contact films may have allowed epoxy adhesive, used to prepare the TEM specimens, to seep into the interface in many locations during sample preparation and may be responsible for the amorphous material at the interface. These issues will be resolved in the near future.

Au/Mg/Au Contacts on Mg:GaN. The ohmic behavior of the Au/Mg/Au contact system on p-GaN contrasts with the rectifying behavior of as-deposited Au contacts. While pure Au was the first layer deposited on the GaN in the sequence, the layer was relatively thin (320 Å) and Mg followed immediately afterward. Cross-sectional TEM samples of both as-deposited and annealed contacts have been sent to our collaborators at ASU for microstructural characterization. It is important to determine the nature of the metal in contact with the GaN surface and whether the proximity of the Mg changes the structure and/or composition of the thin Au layer so as to result in behavior different from that of a thick solid Au contact.

A study of Au/Zn/Au ohmic contacts on Zn-doped GaAs was reported last year by X.W. Lin *et al.* [34]. In contrast to the more familiar Zn/Au contacts for p-GaAs, little or no interfacial reaction with the GaAs surface was seen with annealing when a thin Au layer was deposited on the GaAs first before following with the Zn dopant layer. Au_3Zn phases were found to form at room temperature; no layered structure of the Au/Zn/Au contact system was seen in the as-deposited state. This contact system remained planar and stable even after annealing and did not result in roughening or protrusion formation at the GaAs interface. In this light, it will be informative to characterize both the as-deposited and annealed Au/Mg/Au/p-GaN.

The substantial decrease in ρ_c with increasing measurement temperature is consistent with the thermal ionization of acceptor impurities and consequent increased availability of charge carriers. An Arrhenius-type calculation on the $\rho_c(T)$ data yielded a carrier activation energy of approximately 0.27 eV; this value is close to an estimated value for the Mg acceptor level in GaN reported by Strite and Morkoç in their review of the III-nitride literature [35]. The increase in overall resistance and ρ_c observed as a result of annealing above 650°C may be due to the formation of higher-resistivity compounds. These contacts were deposited in a non-UHV evaporation system; the presence of oxygen may be an issue in this case, particularly with respect to the Mg content. Magnesium is well known for its reactive and easily oxidized behavior. Compositional analysis of the cross-sectional samples will help resolve these issues.

Pt Contacts on Mg:GaN. As has been observed with Al contacts on n-type GaN, the fact that as-deposited Pt contacts on Mg-doped GaN would prove to be ohmic is consistent with the Schottky-Mott-Bardeen model, based on the relationship of the work functions of the two surfaces. Platinum is a very high work function metal (ϕ_{Pt}=5.65 eV) and thus provides a favorable band offset for ohmic contact formation to a p-type semiconductor. In addition, Pt is thermally very stable and highly resistant to oxidation.

The truly linear ohmic behavior and very low ρ_c observed in these measurements are very promising and are the lowest contact resistivities for contacts to p-type GaN reported to date. Investigation of Pt as an ohmic contact candidate for p-type GaN was conducted earlier in this study, as described in the semi-annual report for June 1993, but the results were not as promising at that time. Substantial improvements in GaN film quality and electrical properties have been made since then. The newer Mg:GaN described here were grown by MOVPE instead of MBE, as was the case when the earlier study was conducted. However, it should be pointed out that Mg doping procedures in the MOVPE system at NCSU are still undergoing improvement and optimization, and it is necessary to confirm the type and carrier concentrations in the Mg:GaN films being grown currently. In addition, these results should be compared with Pt contacts deposited using another method besides sputtering, in order to determine how much the ion bombardment experienced during deposition contributed to the observed contact behavior. Annealing studies and upcoming cross-sectional examination will also help assess the value of this promising contact material.

E. Conclusions

The work conducted in this study so far has shown that it is possible to form metal contacts with ohmic, linear I-V behavior and low specific contact resistivity to both n-type and p-type GaN films. The Al contacts on n-type GaN had very good low-resistivity characteristics and remained stable to at least 500°C. The TiN/n-GaN contact system exhibits better performance characteristics than any other investigated in this study to date, and better characteristics than most contacts yet reported for GaN. The Cu_3Ge contacts deposited in a UHV environment have offered very encouraging results and will be undergoing more complete investigation in the coming weeks. Recently, very encouraging results have also been observed with p-type ohmic contacts, particularly with the Pt/Mg:GaN and Au/Mg/Au/Mg:GaN samples. The achievement of as-deposited ohmic contacts to p-GaN is a valuable new development of great importance for device fabrication. Further characterization of these contacts, particularly the microstructural information obtained from X-TEM analysis, will yield greater understanding of the chemical and structural contributions to contact behavior and will allow more rapid and knowledgeable development of improved contact schemes and their capabilities.

F. Future Plans and Goals

In addition to further chemical and structural characterization of the contact systems described in this report, other schemes for improving contact performance will be investigated. One potentially useful approach involves the deposition of high carrier concentration, moderate band gap InN as an interlayer to provide improved band offsets and better carrier transfer across the metal-nitride interface, as proposed by Abernathy *et al.* [31]. Combined with the search for improved contacts to the III-nitrides is the ongoing investigation of Fermi-level pinning and defect states, and the role played by work function and electron affinity differences in contact properties. The evidence examined to date indicates that GaN does indeed experience much less Fermi-level pinning than its more covalently bonded relatives such as GaAs; further work will help to clarify this issue and assist the development of advanced microelectronic and optoelectronic devices.

Another area of study having importance for contact behavior is the issue of surface cleaning and sample preparation. Preliminary investigations of surface cleaning methods by means of XPS analysis have already been performed, and will continue in order to develop a more complete picture of the effects of surface preparation on contact behavior. The role of oxygen and other contaminants at the contact interface is important to understand, and will become even more critical for AlGaN and AlN-based devices due to the strong affinity of Al for oxygen. For such cases the cleanliness of the contact deposition environment will probably be of greater importance as well.

G. References

1. T. C. Shen, G. B. Gao, H. Morkoç, J. Vac. Sci. Technol. B **10**(5) 2113 (1992).
2. R. Williams, *Modern GaAs Processing Techniques* (Artech House, Norwood, MA, 1990)
3. M. Murakami, Materials Science Reports (5) 273 (1990).
4. A. Piotrowska and E. Kaminska, Thin Solid Films **193/194** 511 (1990).
5. A. Piotrowska, A.Guivarc'h and G.Pelous, Solid-St. Electron. **26**(3) 179 (1983).
6. V. L.Rideout, Solid-St. Electron. **18** 541 (1975).
7. K.Tanahashi, H. J. Takata, A.Otsuki and M.Murakami, J. Appl. Phys. **72**(9) 4183 (1992).
8. H.J.Takata, K. Tanahashi, A. Otsuki, H. Inui and M. Murakami, J.Appl. Phys. **72**(9) 4191 (1992).
9. M. C. Hugon, B. Agius, F. Varniere, M. Froment and F. Pillier, J. Appl. Phys. **72**(8) 3570 (1992).
10. W. O. Barnard, G. Myburg and F. D. Auret, Appl. Phys. Lett. **61**(16) 1933 (1992).
11. G. Stareev, Appl. Phys. Lett. **62**(22) 2801 (1993).
12. E. D. Marshall and M. Murakami, in *Contacts to Semiconductors,* edited by L.J. Brillson (Noyes, Park Ridge NJ, 1993).
13. F.W. Ragay, M.R. Leys and J.H. Wolter, Appl. Phys. Lett. **63**(9) 1234 (1993).
14. H.K. Henisch, *Semiconductor Contacts.* (Clarendon Press, Oxford, 1984).
15. E.H. Rhoderick, *Metal-Semiconductor Contacts* (Oxford University Press, New York, 1988).
16. S. Kurtin, T. C. McGill and C. A. Mead, Phys. Rev. Lett. **22**(26) 1433 (1969).

17. J. S. Foresi, *Ohmic Contacts and Schottky Barriers on GaN,* M.S. Thesis, Boston University (1992).
18. J. S. Foresi and T. D. Moustakas, Appl. Phys. Lett. **62**(22) 2859 (1993).
19. B. L. Crowder and S. Zirinski, IEEE Trans. Electron Devices **ED-26**, 369 (1979).
20. S. P. Murarka, *Silicides for VLSI Applications,* Academic Press, New York (1983).
21. L. Krusin-Elbaum, J. Y.-C. Sun, and C.-Y. Ting, IEEE Trans. Electron Devices **ED-34**, 58 (1987).
22. J. C. Hensel, R. T. Tung, J. M. Poate, and F. C. Unterwald, Appl. Phys. Lett. **44**, 913 (1984); Phys. Rev. Lett. **54**, 1840 (1985).
23. P. H. Woerlee, P.M. Th.M. van Attekum, A.A.M. Hoeben, G.A.M. Hurkx, and R.A.M. Wolters, Appl. Phys. Lett. **44**, 876 (1984).
24. M. T. Huang, T. L. Martin, V. Malhotra, and J. E. Mahan, J. Vac. Sci. Technol. B **3**, 836 (1985).
25. L. Krusin-Elbaum and M.O. Aboelfotoh, Appl Phys. Lett. **58**(12) 1341 (1991).
26. M. O. Aboelfotoh, H. M. Tawancy, and L. Krusin-Elbaum, Appl. Phys. Lett. **63**(12) 1622.
27. M. O. Aboelfotoh, K. N. Tu, F. Nava, and M. Michelini, J. Appl. Phys. **75**(1) (1994).
28. M. O. Aboelfotoh, H. M. Tawancy, J. Appl. Phys. **75**(4) (1994).
29. G. K. Reeves and H.B. Harrison, IEEE Electron Device Lett. **EDL-3** 111 (1982).
30. M. E. Lin, Z. Ma, F.Y. Huang, Z.F. Fan, L.H. Allen, and H. Morkoç, Appl. Phys. Lett. **64**(8) 1003 (1994).
31. C. R. Abernathy, S. J. Pearton, F. Ren, and P. W. Wisk, J. Vac. Sci. Technol. B **11**(2) 179 (1993).
32. C. Wang, K. S. Ailey, K. L. More, and R. F. Davis, Inst. Phys. Conf. Ser. No. 137, 417 (1994).
33. D. Korn, H. Pfeifle, and G. Zibold, Z. Physik **270**, 195 (1974).
34. X.W. Lin, Z. Lilienthal-Weber, and J. Washburn, J. Vac. Sci. Technol. B **11**(1) 44 (1993).
35. S. Strite and H. Morkoç, J. Vac. Sci. Technol. B **10**(4) 1237 (1992).

VI. Distribution List

Mr. Max Yoder Office of Naval Research Electronics Division, Code: 314 Ballston Tower One 800 N. Quincy Street Arlington, VA 22217-5660	3
Administrative Contracting Officer Office of Naval Research Regional Office Atlanta 101 Marietta Tower, Suite 2805 101 Marietta Street Atlanta, GA 30332-0490	1
Director, Naval Research Laboratory ATTN: Code 2627 Washington, DC 20375	1
Defense Technical Information Center Bldg. 5, Cameron Station Alexandria, VA 22314	2
Washington Headquarters Services ATTN: Dept. Acctg. Division Room 3B269, The Pentagon Washington, DC 20301-1135	2